DeSilva, D.R., Jones, E.A., Favata, M.F., Jaffee, B.D., Magolda, R.L., Trzaskos, J.M. & Scherle, P.A. (1998) Inhibition of mitogen-activated protein kinase kinase blocks T cell proliferation but does not induce or prevent anergy. *J. Immunol.* **160**, 4175–4181.

Diehl, N.L., Enslen, H., Fortner, K.A., Merritt, C., Stetson, N., Charland, C., Flavell, R.A., Davis, R.J. & Rincon, M. (2000) Activation of the p38 mitogen-activated protein kinase pathway arrests cell cycle progression and differentiation of immature thymocytes *in vivo*. *J. Exp. Med.* **191**, 321–334.

Dinev, D., Jordan, B.W.M., Neufeld, B., Lee, J.D., Lindemann, D., Rapp, U.R. & Ludwig, S. (2001) Extracellular signal regulated kinase 5 (ERK5) is required for the differentiation of muscle cells. *EMBO Rep.* **2**, 829–834.

English, J.M., Pearson, G., Hockenberry, T., Shivakumar, L., White, M.A. & Cobb, M.H. (1999) Contribution of the ERK5/MEK5 pathway to Ras/Raf signaling and growth control. *J. Biol. Chem.* **274**, 31588–31592.

Haskins, K., Kubo, R., White, J., Pigeon, M., Kappler, J. & Marrack, P. (1983) The major histocompatibility complex-restricted antigen receptor on T cells. I. Isolation with a monoclonal antibody. *J. Exp. Med.* **157**, 1149–1169.

Hayashi, M., Kim, S.W., Imanaka-Yoshida, K., Yoshida, T., Abel, E.D., Eliceiri, B., Yang, Y., Ulevitch, R.J. & Lee, J.D. (2004) Targeted deletion of BMK1/ERK5 in adult mice perturbs vascular integrity and leads to endothelial failure. *J. Clin. Invest.* **113**, 1138–1148.

Hirt, B. (1967) Selective extraction of polyoma DNA from infected mouse cell cultures. *J. Mol. Biol.* **26**, 365–369.

Hsu, H.C., Zhou, T. & Mountz, J.D. (2004) Nur77 family of nuclear hormone receptors. *Curr. Drug Targets Inflamm. Allergy* **3**, 413–423.

Kamakura, S., Moriguchi, T. & Nishida, E. (1999) Activation of the protein kinase ERK5/BMK1 by receptor tyrosine kinases. Identification and characterization of a signaling pathway to the nucleus. *J. Biol. Chem.* **274**, 26563–26571.

Kasler, H.G., Victoria, J., Duramad, O. & Winoto, A. (2000) ERK5 is a novel type of mitogen-activated protein kinase containing a transcriptional activation domain. *Mol. Cell. Biol.* **20**, 8382–8389.

Katagiri, Y., Hirata, Y., Milbrandt, J. & Guroff, G. (1997) Differential regulation of the transcriptional activity of the orphan nuclear receptor NGFI-B by membrane depolarization and nerve growth factor. *J. Biol. Chem.* **272**, 31278–31284.

Katagiri, Y., Takeda, K., Yu, Z.X., Ferrans, V.J., Ozato, K. & Guroff, G. (2000) Modulation of retinoid signaling through NGF-induced nuclear export of NGFI-B. *Nat. Cell Biol.* **2**, 435–440.

Kato, Y., Chao, T.H., Hayashi, M., Tapping, R.I. & Lee, J.D. (2000) Role of BMK1 in regulation of growth factor-induced cellular responses. *Immunol. Res.* **21**, 233–237.

Kato, Y., Kravchenko, V.V., Tapping, R.I., Han, J., Ulevitch, R.J. & Lee, J.D. (1997) BMK1/ERK5 regulates serum-induced early gene expression through transcription factor MEF2C. *EMBO J.* **16**, 7054–7066.

Koyasu, S., Suzuki, G., Asano, Y., Osawa, H., Diamantstein, T. & Yahara, I. (1987) Signals for activation and proliferation of murine T lymphocyte clones. *J. Biol. Chem.* **262**, 4689–4695.

Kuang, A.A., Cado, D. & Winoto, A. (1999) Nur77 transcription activity correlates with its apoptotic function *in vivo*. *Eur. J. Immunol.* **29**, 3722–3728.

Li, H., Kolluri, S.K., Gu, J., *et al.* (2000) Cytochrome *c* release and apoptosis induced by mitochondrial targeting of nuclear orphan receptor TR3. *Science* **289**, 1159–1164.

Liu, Z.G., Smith, S.W., McLaughlin, K.A., Schwartz, L.M. & Osborne, B.A. (1994) Apoptotic signals delivered through the T-cell receptor of a T-cell hybrid require the immediate-early gene nur77. *Nature* **367**, 281–284.

Mariathasan, S., Ho, S.S., Zakarian, A. & Ohashi, P.S. (2000) Degree of ERK activation influences both positive and negative thymocyte selection. *Eur. J. Immunol.* **30**, 1060–1068.

Mariathasan, S., Zakarian, A., Bouchard, D., Michie, A.M., Zuniga-Pflucker, J.C. & Ohashi, P.S. (2001) Duration and strength of extracellular signal-regulated kinase signals are altered during positive versus negative thymocyte selection. *J. Immunol.* **167**, 4966–4973.

Masuyama, N., Oishi, K., Mori, Y., Ueno, T., Takahama, Y. & Gotoh, Y. (2001) Akt inhibits the orphan nuclear receptor Nur77 and T-cell apoptosis. *J. Biol. Chem.* **276**, 32799–32805.

Nakaoka, Y., Nishida, K., Fujio, Y., Izumi, M., Terai, K., Oshima, Y., Sugiyama, S., Matsuda, S., Koyasu, S., Yamauchi-Takihara, K., Hirano, T., Kawase, I. & Hirota, H. (2003) Activation of gp130 transduces hypertrophic signal through interaction of scaffolding–docking protein Gab1 with tyrosine phosphates SHP2 in cardiomyocytes. *Circ. Res.* **93**, 221–229.

Nishida, E. & Gotoh, Y. (1993) The MAP kinase cascade is essential for diverse signal transduction pathways. *Trends Biochem. Sci.* **18**, 128–131.

Nishimoto, S., Kusakabe, M. & Nishida, E. (2005) Requirement of the MEK5–ERK5 pathway for neural differentiation in *Xenopus* embryonic development. *EMBO Rep.* **6**, 1064–1069.

Pang, L., Sawada, T., Decker, S.J. & Saltiel, A.R. (1995) Inhibition of MAP kinase kinase blocks the differentiation of PC-12 cells induced by nerve growth factor. *J. Biol. Chem.* **270**, 13585–13588.

Regan, C.P., Li, W., Boucher, D.M., Spatz, S., Su, M.S. & Kuida, K. (2002) Erk5 null mice display multiple extraembryonic vascular and embryonic cardiovascular defects. *Proc. Natl. Acad. Sci. USA* **99**, 9248–9253.

Rincon, M., Whitmarsh, A., Yang, D.D., Weiss, L., Derijard, B., Jayaraj, P., Davis, R.J. & Flavell, R.A. (1998) The JNK pathway regulates the *in vivo* deletion of immature CD4+CD8+ thymocytes. *J. Exp. Med.* **188**, 1817–1830.

Sakaue, M., Adachi, H., Dawson, M. & Jetten, A.M. (2001) Induction of Egr-1 expression by the retinoid AHPN in human lung carcinoma cells is dependent on activated ERK1/2. *Cell Death Differ.* **8**, 411–424.

Sasaki, T., Kojima, H., Kishimoto, R., Ikeda, A., Kunimoto, H. & Nakajima, K. (2006) Spatiotemporal regulation of c-Fos by ERK5 and the E3 ubiquitin ligase UBR1, and its biological role. *Mol. Cell* **24**, 63–75.

Schaeffer, H.J. & Weber, M.J. (1999) Mitogen-activated protein kinases: Specific messages from ubiquitous messengers. *Mol. Cell. Biol.* **19**, 2435–2444.

Sohn, S.J., Li, D., Lee, L.K. & Winoto, A. (2005) Transcriptional regulation of tissue-specific genes by ERK5 mitogen-activated protein kinase. *Mol. Cell. Biol.* **25**, 8553–8566.

Sugawara, T., Moriguchi, T., Nishida, E. & Takahama, Y. (1998) Differential roles of ERK and p38 MAPK pathways in positive and negative selection of T lymphocytes. *Immunity* **9**, 565–574.

Winoto, A. & Littman, D.R. (2002) Nuclear hormone receptors in T lymphocytes. *Cell* **109**, S57–S66.

Woronicz, J.D., Calnan, B., Ngo, V. & Winoto, A. (1994) Requirement for the orphan steroid receptor Nur77 in apoptosis of T-cell hybridomas. *Nature* **367**, 277–281.

Woronicz, J.D., Lina, A., Calnan, B.J., Szychowski, S., Cheng, L. & Winoto, A. (1995) Regulation of the Nur77 orphan steroid receptor in activation-induced apoptosis. *Mol. Cell. Biol.* **15**, 6364–6376.

Yazdanbakhsh, K., Choi, J.W., Li, Y., Lau, L.F. & Choi, Y. (1995) Cyclosporin A blocks apoptosis by inhibiting the DNA binding activity of the transcription factor Nur77. *Proc. Natl. Acad. Sci. USA* **92**, 437–441.

Yonezawa, N., Nishida, E., Sakai, H., Koyasu, S., Matsuzaki, F., Iida, K. & Yahara, I. (1988) Purification and characterization of the 90-kDa heat-shock protein from mammalian tissues. *Eur. J. Biochem.* **177**, 1–7.

Youn, H.D., Sun, L., Prywes, R. & Liu, J.O. (1999) Apoptosis of T cells mediated by calcium-induced release of the transcription factor MEF2. *Science* **286**, 790–793.

Zhou, T., Cheng, J., Yang, V., Wang, Z., Liu, C., Su, X., Bluethmann, H. & Mountz, J.D. (1996) Inhibition of Nur77/Nurr1 leads to inefficient clonal deletion of self-reactive T cells. *J. Exp. Med.* **183**, 1879–1892.

Received: 23 June 2007
Accepted: 17 January 2008

Mammalian target of rapamycin and glycogen synthase kinase 3 differentially regulate lipopolysaccharide-induced interleukin-12 production in dendritic cells

Masashi Ohtani,[1,2] Shigenori Nagai,[1,2] Shuhei Kondo,[1] Shinta Mizuno,[1] Kozue Nakamura,[1] Masanobu Tanabe,[3] Tsutomu Takeuchi,[3] Satoshi Matsuda,[1,2] and Shigeo Koyasu[1,2]

[1]Department of Microbiology and Immunology, Keio University School of Medicine, Tokyo; [2]Core Research for Evolutional Science and Technology, Japan Science and Technology Agency, Saitama; and [3]Department of Tropical Medicine and Parasitology, Keio University School of Medicine, Tokyo, Japan

Phosphoinositide 3-kinase (PI3K) negatively regulates Toll-like receptor (TLR)–mediated interleukin-12 (IL-12) expression in dendritic cells (DCs). We show here that 2 signaling pathways downstream of PI3K, mammalian target of rapamycin (mTOR) and glycogen synthase kinase 3 (GSK3), differentially regulate the expression of IL-12 in lipopolysaccharide (LPS)–stimulated DCs. Rapamycin, an inhibitor of mTOR, enhanced IL-12 production in LPS-stimulated DCs, whereas the activation of mTOR by lentivirus-mediated transduction of a constitutively active form of Rheb suppressed the production of IL-12. The inhibition of protein secretion or deletion of IL-10 cancelled the effect of rapamycin, indicating that mTOR regulates IL-12 expression through an autocrine action of IL-10. In contrast, GSK3 positively regulates IL-12 production through an IL-10–independent pathway. Rapamycin-treated DCs enhanced Th1 induction in vitro compared with untreated DCs. LiCl, an inhibitor of GSK3, suppressed a Th1 response on *Leishmania major* infection in vivo. These results suggest that mTOR and GSK3 pathways regulate the Th1/Th2 balance though the regulation of IL-12 expression in DCs. The signaling pathway downstream of PI3K would be a good target to modulate the Th1/Th2 balance in immune responses in vivo. (Blood. 2008; 112:635-643)

Introduction

Dendritic cells (DCs) recognize pathogens via pattern-recognition receptors, such as Toll-like receptors (TLRs), nucleotide-binding oligomerization domain (NOD)-like receptors, and retinoic acid inducible gene-1 (RIG-I)-like receptors, produce various cytokines, including interleukin-12 (IL-12), and thus activate the innate immune system, which in turn leads to the induction of adaptive immunity.[1-5] Bioactive IL-12 is composed of p40 and p35 subunits and functions as a crucial inducer of Th1 responses. IL-12 is typically produced by antigen-presenting cells such as DCs and monocytes-macrophages and plays an important role in infection and tumor immunity.[1-5] Because the overproduction of IL-12 gives rise to strong cell-mediated immunity and organ-specific autoimmune diseases via exaggerated Th1 cell differentiation, it is critical that IL-12 levels be tightly controlled.[5]

Phosphoinositide 3-kinases (PI3Ks) are lipid kinases playing important roles in various signal transduction pathways.[6] PI3K family members are classified into 4 subgroups according to their structure and substrate specificity. Among them, class IA heterodimeric PI3Ks are involved in receptor-mediated signaling pathways in the immune system.[6,7] Phosphatidylinositol-(3,4)bisphosphate and phosphatidylinositol(3,4,5)trisphosphate produced by class IA PI3Ks recruit specific signaling proteins containing a pleckstrin homology domain to the plasma membrane. These proteins include Akt and phosphoinositide-dependent kinase 1 and are involved in a wide range of cellular responses, such as cell growth, survival, and cytokine production.[6,7] PI3K signaling pathways are counteracted by phosphatase and tensin homologue deleted on chromosome 10 (PTEN), a 3-phosphoinositide–specific lipid phosphatase.[6]

We have previously demonstrated that PI3K negatively regulates IL-12 production in DCs stimulated with TLR ligands.[8,9] An enhanced Th1 response was observed on *Leishmania major* infection,[8] and an impaired Th2 response was observed on *Strongyloides venezuelensis* infection[10] in mice deficient for p85α, a major regulatory subunit of class IA PI3K, indicating that PI3K plays a key role in the regulation of Th1/ Th2 balance in vivo. Although several reports confirmed the negative feedback regulation of IL-12 production by PI3K on TLR stimulation,[11-13] the molecular mechanism(s) remains controversial.

One downstream substrate of PI3K pathways is a Ser/Thr protein kinase named "mammalian target of rapamycin" (mTOR), which regulates cell growth and protein synthesis by activating p70 S6 kinase (p70S6K) and by inhibiting eukaryotic initiation factor 4E-binding protein 1 (4E-BP1).[14] There are 2 functionally distinct mTOR complexes, mTORC1 and mTORC2, and only mTORC1 acts downstream of the PI3K-Akt-tuberous sclerosis complex 2 (TSC2)–Rheb signaling pathway to phosphorylate p70S6K and 4E-BP1 in a rapamycin-sensitive fashion[14] (Figure 1A). Although the mTOR pathway is activated in response to not only growth factors but also environmental stresses such as hypoxia,[14] the TLR-triggered mTOR function is poorly understood. In the present study, we show that mTOR negatively regulates IL-12 production through the production of IL-10 in DCs. We further demonstrate that glycogen synthase kinase 3 (GSK3), another downstream target of PI3K pathways, is also involved in the PI3K-mediated regulation of IL-12 production in a manner distinct from that of mTOR. We also provide evidence that the inhibition of mTOR and

Submitted February 1, 2008; accepted April 9, 2008. Prepublished online as *Blood* First Edition paper, May 20, 2008; DOI 10.1182/blood-2008-02-137430.

The online version of this article contains a data supplement.

The publication costs of this article were defrayed in part by page charge payment. Therefore, and solely to indicate this fact, this article is hereby marked "advertisement" in accordance with 18 USC section 1734.

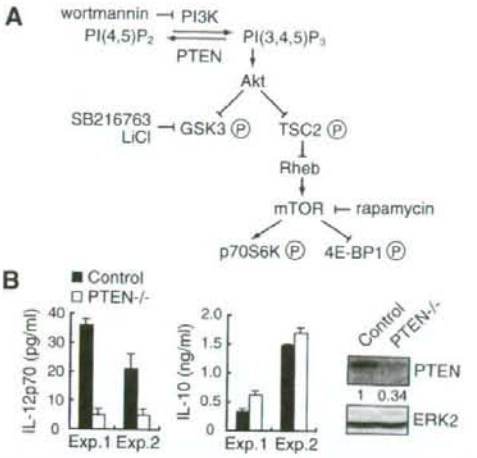

Figure 1. LPS-induced IL-12 production is suppressed in PTEN$^{-/-}$ BMDCs. (A) The overview of PI3K signaling pathway. $PI(4,5)P_2$ indicates phosphatidylinositol(4,5)bisphosphate; $PI(3,4,5)P_3$, phosphatidylinositol-(3,4,5)trisphosphate. (B) BMDCs from PTEN$^{-/-}$ mice (n = 2) or their littermate controls (n = 2) were stimulated with 1 μg/mL LPS for 24 hours and assayed for the production of IL-12p70 and IL-10 by ELISA. Data are indicated as median plus or minus SD. Essentially, the same results were obtained with 2 independent experiments (experiments 1 and 2). The expression levels of PTEN and ERK2 in BMDCs were determined by Western blotting (right panel).

GSK3 pathways in DCs results in the increase and decrease of Th1 responses, respectively.

Methods

Reagents

Lipopolysaccharide (LPS) from *Escherichia coli* 055:B5 was purchased from Sigma-Aldrich (St Louis, MO). Recombinant human (rh) GM-CSF, rhIL-4, rhIL-10, and recombinant mouse (rm) GM-CSF were purchased from PeproTech (Rocky Hill, NJ). Wortmannin, rapamycin, SB216763, cycloheximide, and brefeldin A (BFA) were purchased from Calbiochem (San Diego, CA). Antibodies to ERK2, IκBα, p70S6K, Rheb, GSK3α/β, and STAT3 were purchased from Santa Cruz Biotechnology (Santa Cruz, CA). Antibody to Akt and phosphorylation-specific antibodies to Akt (Ser473), GSK3α/β (Ser21/Ser9), TSC2 (Thr1462), p38 (Thr180/Tyr182), ERK (Thr202/Tyr204), JNK (Thr183/Tyr185), and STAT3 (Tyr705) were purchased from Cell Signaling Technology (Danvers, MA).

Mice

C57BL/6 and BALB/c mice were purchased from Nihon SLC. IL-10$^{-/-}$ mice on a C57BL/6 background were purchased from The Jackson Laboratory (Bar Harbor, ME). Mice deficient for p85α were reported previously.[15,16] Mice had been backcrossed to the BALB/c background for 12 generations. STAT3 mutant (LysM-Cre x STAT3$^{flox/flox}$) mice[17] on a mixed (129 × C57BL/6) background were kindly provided by Dr K. Takeda (Osaka University, Osaka, Japan). STAT3$^{flox/flox}$ or LysM-Cre x STAT3$^{flox/+}$ mice were used as controls. PTEN mutant (LysM-Cre x PTEN$^{flox/flox}$) mice[18,19] on a C57BL/6 background were kindly provided by Dr A. Suzuki (Akita University, Akita, Japan). PTEN$^{flox/flox}$ mice were used as controls. LysM-Cre x STAT3$^{flox/flox}$ and LysM-Cre x PTEN$^{flox/flox}$ mice were referred to here as STAT3$^{-/-}$ and PTEN$^{-/-}$ mice, respectively. Mice were maintained at Taconic Farms (Germantown, NY) or in our animal facility under specific pathogen-free conditions. All experiments were performed in accordance with our institutional guidelines.

Preparation of dendritic cells

To generate bone marrow (BM)–derived DCs (BMDCs), mouse BM cells were cultured at 10^6/mL in complete medium (RPMI 1640; Sigma-Aldrich, 10% fetal calf serum, 55 μM 2-mercaptoethanol, 100 U/mL penicillin, 100 μg/mL streptomycin) supplemented with 10 ng/mL rmGM-CSF for 6 days. The culture medium was changed every 2 days. On day 6, BMDCs were isolated using antimouse CD11c magnetic beads (Miltenyi Biotec, Auburn, CA) with an AutoMACS (Miltenyi Biotec). Human peripheral blood mononuclear cells from normal healthy volunteers were isolated by centrifugation on a Ficoll-Metrizoate density gradient (Lymphoprep; Nycomed, Oslo, Norway). The protocol was approved by the local ethics committee at Keio University School of Medicine, and informed consent was obtained from donors in accordance with the Declaration of Helsinki. Monocytes were then isolated using antihuman CD14 magnetic beads (Miltenyi Biotec) with an AutoMACS, followed by incubation at 10^6 cells/mL in complete medium supplemented with 100 ng/mL rhGM-CSF and 100 ng/mL rhIL-4 for 6 days, to obtain monocyte-derived DCs (MDDCs).

Western blotting

Western blotting was carried out as described.[8] To detect phospho-STAT3 and phospho-TSC2, immunoreaction enhancer (Can Get Signal, Toyobo, Japan) was added to the reaction according to the manufacturer's instructions. ERK2 was used as a loading control. A LAS-3000 imaging system (Fuji) was used to produce digital images. Signal intensities (for phospho-STAT3) and signal profiles (for p70S6K) were quantified with Image Gauge software version 4.1 (Fuji).

Enzyme-linked immunosorbent assay

Cytokine concentrations in the culture supernatants were quantified by enzyme-linked immunosorbent assay (ELISA; Quantikine; R&D Systems, Minneapolis, MN).

Quantitative real-time polymerase chain reaction

Total RNA was prepared using NucleoSpin RNA II (Macherey-Nagel, Düreu, Germany), and cDNA was synthesized with Ready-To-Go T-Primed First-Strand kit (GE Healthcare, Chalfont St Giles, United Kingdom). Quantitative real-time polymerase chain reaction (PCR) was performed by applying the real-time SYBR Green PCR technology using SYBR premix Ex Taq (Takara, Otsu, Japan) with specific primers on an iCycler IQ (Bio-Rad, Hercules, CA). PCR cycling was as follows: 95°C for 10 seconds for 1 cycle, 95°C for 5 seconds, 58°C for 20 seconds, 72°C for 15 seconds for 40 cycles, and 70°C for 5 minutes. Amplification of cyclophilin A mRNA was done for each sample as an endogenous control. Primer pairs specific for IL-12p40 (forward, CAGAAGCTAACCATCTCCTGGTTTG; reverse, CCGGAGTAATTTGGTGCTCCACAC), IL-12p35 (forward, TCACATCTCATCTCCCCAAA; reverse, TCTGCTAACACATTGAGGGG), IL-10 (forward, GGTTGCC-AAGCCTTATCGGA; reverse, ACCTGCTCCACTGCCTTGCT), interferon-β (IFN-β) (forward, CCATCCAAGAGATGCTCCAG; reverse, GTGGAGAGCAGTTGAGGACA), suppressor of cytokine signaling 3 (SOCS3) (forward, GGGGGAGGCAGGAGGTGATGGA; reverse, GGGCGGGCTGGAGGTGGATT) and cyclophilin A (forward, ATGGCACTGGCGGCAGGTCC; reverse, TTGCCATTCCTGGACCCAAA) were used.

Preparation of lentiviral vectors

The following constructs were kindly provided by Dr H. Miyoshi (RIKEN, Tsukuba, Japan): CSII-EF-MCS-IRES2-Venus, a self-inactivating lentiviral construct; pCAG-HIVgp and pCMV-VSVG-RSV-Rev, packaging constructs.[20] This lentiviral system is designed to express a desired gene under the direction of the elongation factor-1 promoter along with internal ribosomal entry site (IRES)-driven Venus, a derivative of YFP,[21] as a marker for monitoring the infection efficiency. Mouse Rheb was amplified by PCR using cDNA from the brain of C57BL/6 mice as a template (5′

primer, ATGCCTCAGTCCAAGTCCCG; 3′ primer, TCACATCACCGAGCACGAAG) and cloned into the pGEM-T Easy vector (Promega, Madison, WI). After sequence verification, the construct was subjected to PCR mutagenesis to obtain Rheb Q64L, a constitutively active form of Rheb, Glu-64 replaced by Leu. The product was verified by DNA sequencing and subcloned into CSII-EF-MCS-IRES2-Venus. For the generation of lentiviral vectors, 293T cells were transfected with CSII-EF-MCS-IRES2-Venus with or without Rheb Q64L insert, pCAG-HIVgp, and pCMV-VSUG-RSV-Rev using Lipofectamine 2000 (Invitrogen, Carlsbad, CA). After 2 days, culture supernatants were passed through a 0.45-μm filter, condensed to 0.5% volume, and used for gene transduction.

Generation of gene-transduced BMDCs

Mouse BM cells were incubated with phycoerythrin-conjugated antibodies against CD3ε, CD4, CD8α, CD11b, Gr-1, B220, and TER119 (BD Biosciences, San Jose, CA) along with anti-phycoerythrin microbeads (Miltenyi Biotec), followed by negative selection with an AutoMACS. The remaining cells (0.5×10^5 cells/0.5 mL) were cultured with 10 ng/mL rmGM-CSF in a 24-well plate for 2 days, followed by spin infection (1800 rpm, 2 hours) with 40 μL of each viral vector along with 5 μg/mL polybrene. After infection, each well was split into 2 wells (2 mL/well) and cultured with 10 ng/mL rmGM-CSF for another 4 days. The culture medium was changed every 2 days. The cells were then harvested, washed, and incubated with allophycocyanin-conjugated antimouse CD11c monoclonal antibody (mAb), and Venus-as well as CD11c-positive cells were sorted as gene-transduced BMDCs using a FACSAria (BD Biosciences). The purity was estimated to be more than 85%.

$CD4^+$ T-cell priming

Human MDDCs (1×10^6 cells) were incubated in the presence or absence of 10 μg/mL tuberculin purified protein derivative (PPD) for 1 hour, and subsequently stimulated with or without 1 μg/mL of LPS along with or without 100 nM of rapamycin. After 2 hours of stimulation, the cells were harvested, washed, and cultured (3×10^5 cells) for a week with $CD4^+$ T cells from the same donor (3×10^6 cells), which were isolated from peripheral blood mononuclear cells using antihuman CD4 magnetic beads (Miltenyi Biotec) with an AutoMACS. $CD4^+$ T cells were then restimulated with antihuman CD3ε (10 μg/mL) and antihuman CD28 (1 μg/mL) mAbs for 48 hours.

Leishmania major infection

L major infection was performed as described.[8,22] Two days after infection, 40 μL of 2 mM LiCl/phosphate-buffered saline (PBS) or PBS were injected into the infected left hind footpad subcutaneously.

Results

Products of PI3K are involved in the regulation of IL-12 expression

To prove that the lipid kinase activity of PI3K regulates IL-12 production, we examined the role of PTEN, which catalyzes a reaction opposite to PI3K (Figure 1A). BMDCs lacking PTEN produced lower amounts of IL-12 than control BMDCs on LPS stimulation (Figure 1B), indicating that the products of PI3Ks, phosphatidylinositol(3,4,5)trisphosphate in particular, are indeed critical for the regulation of IL-12 expression.

Activation of mTOR and GSK3 pathways by LPS stimulation of DCs

We examined the signaling components of PI3K-Akt pathway in LPS-stimulated BMDCs (Figure 1A). As shown in Figure 2, LPS stimulation induced the phosphorylation of TSC2 and GSK3,

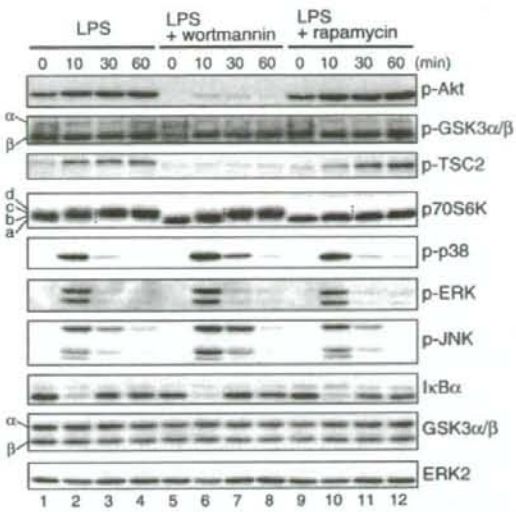

Figure 2. The PI3K signaling pathway is activated by LPS in BMDCs. BMDCs were cultured overnight and then pretreated with either 100 nM wortmannin or 10 ng/mL rapamycin for 20 minutes or left untreated before being stimulated with 1 μg/mL LPS for the indicated times. Cell lysates were analyzed for phospho-Akt, phospho-GSK3α/β, phospho-TSC2, p70S6K, phospho-p38, phospho-ERK, phospho-JNK, IκBα, GSK3α/β, and ERK2 by Western blotting. Four dots added between the 10-minute and 30-minute lanes of p70S6K samples indicate the migration positions of hyperphosphorylated p70S6K caused by multiple phosphorylation events, which are represented as a through d on the left side (Figure S1).

known targets of Akt. The activation of mTOR was evaluated by the phosphorylation of p70S6K. Consistent with the fact that mTOR is activated by serum and nutrients, p70S6K was partially phosphorylated even without LPS (Figure 2 lane 1). The hyperphosphorylation of p70S6K examined by electrophoretic mobility shifts was induced within 10 minutes (Figure 2 lane 2) and became clearer up to 60 minutes after LPS stimulation (Figure 2 and Figure S1 lane 4, available on the *Blood* website; see the Supplemental Materials link at the top of the online article; note that the electrophoretic mobility of p70S6K shifts from a and b up to c and d bands). Rapamycin completely blocked the phosphorylation of p70S6K (Figures 2, S1, compare lanes 1-4 and 9-12). In contrast, rapamycin had no effect on the LPS-induced phosphorylation of Akt and TSC2 (Figure 2 lanes 9-12), which is consistent with the fact that Akt and TSC2 act upstream of mTOR (Figure 1A). Wortmannin, an inhibitor of PI3K, only partially blocked the LPS-induced phosphorylation of p70S6K (Figures 2, S1, lanes 5-8), whereas the phosphorylation of Akt and TSC2 was completely inhibited (Figure 2 lanes 5-8). These data suggest that LPS-induced mTOR activation is mediated by both PI3K-dependent and-independent pathways, the latter of which could involve serum and/or nutrients.

GSK3 activity is negatively regulated by Akt-mediated phosphorylation.[23] We found that GSK3β was predominantly phosphorylated on LPS stimulation in BMDCs, whereas both GSK3α and GSK3β were expressed (Figure 2 lanes 1-4). The effect of wortmannin on GSK3β phosphorylation was partial (Figure 2 lanes 5-8), indicating that the LPS-induced phosphorylation of GSK3β was also mediated by both PI3K-dependent and -independent pathways. As expected, rapamycin had no effect on the LPS-induced phosphorylation of GSK3β (Figure 2 lanes 9-12).

We also examined the effects of rapamycin and wortmannin on LPS-activated MAPK and NF-κB pathways. Rapamycin had little effect on the phosphorylation status of MAPK family members or the degradation of IκBα, a measure of NF-κB activation (Figure 2, compare lanes 1-4 and lanes 9-12). In contrast, consistent with previous reports,[8,24,25] wortmannin slightly but reproducibly enhanced the LPS-induced phosphorylation of p38 as well as JNK (Figure 2, compare lanes 3 and 7), indicating that a PI3K-dependent but mTOR-independent pathway(s) negatively regulates the activation of p38 and JNK. Wortmannin had little effect on IκBα degradation, indicating that the NF-κB pathway is probably not the target of PI3K pathway in BMDCs.

Rapamycin augments LPS-induced IL-12 production but suppresses IL-10 production in an mTOR-dependent manner

We next examined the role of mTOR in the regulation of IL-12 expression. As shown in Figure 3A, the treatment of BMDCs with rapamycin as well as wortmannin enhanced LPS-induced IL-12p70 production. In contrast, LPS-induced IL-10 production was suppressed by rapamycin or wortmannin, and the effect of rapamycin was more potent than wortmannin (Figure 3A). Rapamycin had the same effect on human MDDCs (Figure S2). On the other hand, rapamycin and wortmannin had little effect on the production of IL-6 and tumor necrosis factor-α (TNF-α; Figure 3A). PTEN$^{-/-}$ BMDCs produced slightly more IL-10 compared with control BMDCs (Figure 1B), but the effect of PTEN deficiency is more pronounced on IL-12 compared with IL-10 production.

A complex of rapamycin and FK506-binding protein 12 (FKBP12) binds to and inhibits mTOR. Because FK506 competes with rapamycin for binding to FKBP12, the excess amounts of FK506 cancel the biologic actions of the rapamycin-FKBP12 complex.[26] Indeed, FK506 prevented the rapamycin-induced augmentation of IL-12p70 and IL-12p40 production in a dose-dependent manner (Figure 3B). The suppression of IL-10 production by rapamycin was also canceled with excess FK506 (Figures 3B, S3). Excess amounts of FK506 partially restored the hyperphosphorylation of p70S6K (Figure S3). These results confirm that the effect of rapamycin on cytokine production is mediated by the inhibition of mTOR function.

We further examined the effects of wortmannin and rapamycin on LPS-induced cytokine mRNA expression, including IL-12p40, IL-12p35, IL-10, and IFN-β by real-time RT-PCR (Figure 3C). Consistent with these results, the expression of both IL-12p40 and IL-12p35 mRNAs was enhanced by wortmannin and rapamycin. In contrast, IL-10 mRNA expression was suppressed only by rapamycin. Interestingly, wortmannin but not rapamycin enhanced LPS-induced IFN-β mRNA expression. These results collectively suggest that the PI3K regulates the expression of distinct sets of cytokine genes expression in mTOR-dependent and -independent pathways.

Constitutively active Rheb affects the regulation of cytokine production

To further confirm the role of mTOR in cytokine gene regulation, we used a lentiviral vector-mediated gene delivery system[20] to activate mTOR by expressing a constitutively active form of Rheb (Rheb Q64L).[27] The phosphorylation-induced electrophoretic mobility shift of p70S6K in untreated and LPS-stimulated DCs was augmented in BMDCs expressing Rheb Q64L compared with control BMDCs (Figure 4A and Figure S4 lanes 1 and 3, lanes 2 and 4), confirming the activity of Rheb Q64L. As shown in Figure

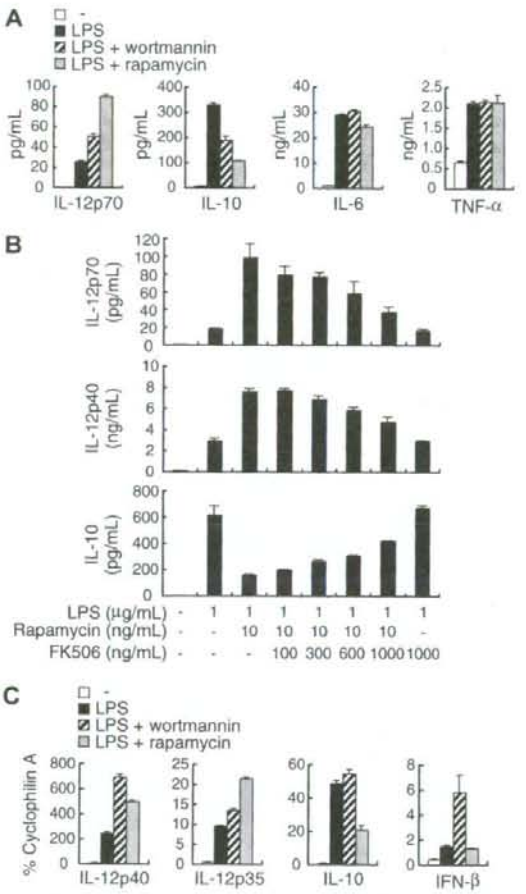

Figure 3. The effect of rapamycin on LPS-induced cytokine expression in BMDCs. (A) BMDCs were stimulated with 1 μg/mL LPS in the presence or absence of either 100 nM wortmannin or 10 ng/mL rapamycin for 24 hours and assayed for the production of IL-12p70, IL-10, IL-6, and TNF-α by ELISA. (B) BMDCs were stimulated with 1 μg/mL LPS with or without 10 ng/mL rapamycin along with the indicated concentrations of FK506 for 24 hours and assayed for the production of IL-12p70, IL-12p40, and IL-10 by ELISA. (C) BMDCs were pretreated with or without either 100 nM wortmannin or 10 ng/mL rapamycin for 20 minutes before stimulation with 1 μg/mL LPS. After 4 hours, total RNA was isolated, and IL-12p40, IL-12p35, IL-10, and IFN-β mRNA levels were assessed by real-time PCR using cyclophilin A mRNA as a reference. All data are indicated as median plus or minus SD of duplicate samples. Similar results were obtained with 2 to 4 independent experiments.

4B, LPS-induced IL-12p70 production was decreased in Rheb Q64L-expressing BMDCs compared with mock-infected BMDCs. In contrast, LPS-induced IL-10 production was increased in Rheb Q64L-expressing BMDCs. No difference in IL-6 production was observed (data not shown). These results indicate that mTOR is indeed involved in the regulation of IL-12 and IL-10 production in LPS-stimulated BMDCs.

The effect of rapamycin on IL-12 expression involves IL-10 in an autocrine manner

Because mTOR is involved in diverse biologic processes, including protein synthesis and gene expression,[14] it is possible that mTOR regulates IL-12 gene expression through new protein synthesis. When BMDCs were treated with cycloheximide to inhibit de novo

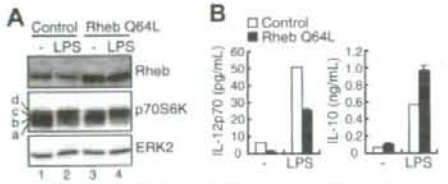

Figure 4. The effect of Rheb Q64L on LPS-induced cytokine production. BMDCs were infected with a lentivirus vector expressing a constitutively active form of Rheb (Rheb Q64L) or vector alone (control). Gene-transduced BMDCs were isolated ("Methods") and stimulated with or without 1 μg/mL LPS for 24 hours. (A) The cell lysates were analyzed for Rheb, p70S6K, and ERK2 by Western blotting. Note that the mobility shifts of p70S6K caused by multiple phosphorylation are represented as a through d (Figure S4). (B) The production of IL-12p70 and IL-10 in culture supernatants was assayed by ELISA.

protein synthesis, the effect of rapamycin was reduced (data not shown). BFA, which blocks protein secretion, abrogated the effect of rapamycin on LPS-induced IL-12p40 and IL-12p35 mRNA expression (Figure 5A). These results strongly suggest that rapamycin controls LPS-induced IL-12 expression through a newly synthesized autocrine mediator(s).

IL-10 is an anti-inflammatory cytokine capable of inhibiting the LPS-induced production of proinflammatory cytokines, including IL-12 in DCs.[28] When we examined the kinetics of LPS-induced IL-12 and IL-10 expression, rapamycin augmented IL-12p40 and IL-12p35 mRNA expression at 4 hours but not 2 hours after LPS stimulation (Figure 5B). On the other hand, the rapamycin-induced suppression of IL-10 mRNA expression was already observed at 2 hours after LPS stimulation (Figure 5B). Consistent with these results, LPS-induced IL-10 production evaluated by ELISA was significantly reduced by rapamycin at 4 hours after LPS stimulation, whereas IL-12p40 production was little affected (data not shown). These results suggest that the suppression of IL-10 expression by rapamycin subsequently augments IL-12 expression.

To test this hypothesis further, we examined whether rapamycin attenuates the IL-10 signaling pathway in LPS-stimulated DCs. For this purpose, we analyzed the phosphorylation status of STAT3 at Tyr705 as a measure of IL-10 signaling. We found that the tyrosine phosphorylation of STAT3 was markedly induced at 2 hours after LPS stimulation, which was inhibited by rapamycin (Figure 5C). Similar results were obtained in human MDDCs (Figure S5). To rule out the possibility that rapamycin directly inhibits the STAT3 signaling pathway, we examined the effect of rapamycin on the IL-10–induced expression of SOCS3, a well-known target of the STAT3 signaling pathway.[29] As shown in Figure 5D, SOCS3 mRNA expression induced by IL-10 stimulation was unaffected by rapamycin. Collectively, these results indicate that rapamycin directly suppresses LPS-induced IL-10 expression but not the STAT3 signaling pathway.

To confirm that rapamycin works through the IL-10-STAT3 pathway to down-regulate IL-12 expression, we used IL-10$^{-/-}$ and STAT3$^{-/-}$ DCs. As shown in Figure 5E, the effect of rapamycin was virtually absent in IL-10$^{-/-}$ BMDCs (1.2 ± 0.03-fold increase) compared with WT BMDCs (3.8 ± 0.1-fold increase). Essentially the same result was obtained with STAT3$^{-/-}$ BMDCs (Figure 5F, 3.3 ± 0.2-fold increase in control BMDCs vs 1.2 ± 0.1-fold increase in STAT3$^{-/-}$ BMDCs). The production of IL-12p70 from IL-10$^{-/-}$ DCs was strongly suppressed by the addition of exogenous IL-10, and such inhibition was rapamycin-independent (Figure S6). These results clearly indicate that rapamycin enhances IL-12 production through the inhibition of autocrine IL-10 action in LPS-stimulated BMDCs.

mTOR and GSK3 cooperatively regulate LPS-induced IL-12 production

As wortmannin had only a marginal effect on LPS-induced phosphorylation of p70S6K (Figure 2) as well as IL-10 expression (Figure 3A,C), we examined pathways other than mTOR that lie downstream of PI3K. Indeed, GSK3 has been reported to regulate the TLR-mediated production of cytokines, such as IL-12p40 and IL-10 in human monocytes and DCs.[30,31] We therefore examined whether GSK3 regulates LPS-induced cytokine production in mouse BMDCs using SB216763, a specific GSK3 inhibitor. SB216763 attenuated IL-12p70 production but enhanced IL-10 production by LPS-stimulated DCs (Figure 6A, lane 5). We obtained similar results with another GSK3 inhibitor LiCl (data not shown). These data indicate that PI3K regulates IL-12 production through both mTOR and GSK3 pathways and that GSK3 positively regulates LPS-induced IL-12p70 and negatively regulates IL-10 production in BMDCs.

Given that the PI3K-Akt pathway negatively regulates GSK3 (Figure 1A), the treatment of cells with wortmannin should activate GSK3. Interestingly, wortmannin augmented the effect of rapamycin on LPS-induced IL-12p70 production (Figure 6A lanes 2-4 and 6). On the other hand, consistent with the marginal effect of wortmannin alone (Figure 6A lane 3), wortmannin failed to augment the suppressive effect of rapamycin on LPS-induced IL-10 production (Figure 6A lanes 2-4 and 6), suggesting that mTOR and GSK3 differentially regulate IL-12 production. Wortmannin had little effect on LPS-induced IL-12p70 and IL-10 production in the presence of SB216763 (Figure 6A lanes 5 and 7). It is probable that the contribution of GSK3 is similar to or greater than that of mTOR for the regulation of IL-12 production in DCs. Consistent with those observations, LPS-induced IL-12p70 production was decreased in the presence of SB216763 in IL-10$^{-/-}$ BMDCs (Figure 6B). These results collectively indicate that GSK3 directly regulates LPS-induced IL-12 production independent of IL-10 (Figure 6C).

Attenuation of mTOR and GSK3 affects Th1/Th2 balance

Because IL-12 is critical for triggering Th1 responses, our results raise an interesting possibility that blocking mTOR and GSK3 may enhance and diminish Th1 responses, respectively. Human peripheral CD4$^+$ T cells stimulated with MDDCs pretreated with LPS plus PPD in the presence of rapamycin produced more IFN-γ on restimulation with anti-CD3 plus anti-CD28 antibodies than CD4$^+$ T cells stimulated with DCs pretreated in the absence of rapamycin (Figure 7A). It is thus probable that treatment of DCs with rapamycin results in the augmentation of a Th1 response presumably through enhanced IL-12 production and reduced IL-10 production. We next examined the effect of GSK3 inhibition in an in vivo infection model with *L major*, in which adequate Th1 development is required for disease control.[22] We have previously shown that Th2 prone BALB/c mice can elicit a reasonable Th1 response on *L major* infection in the absence of p85α (Fukao et al[8] and Figure 7B, compare open triangles and open circles). Because GSK3 is expected to have an increased activity in the absence of p85α, we administered a GSK3 inhibitor, LiCl, into footpad of p85α$^{-/-}$ mice on a BALB/c background when infected with *L major*. As shown in Figure 7B, whereas p85α$^{-/-}$ BALB/c mice were resistant to infection, the administration of LiCl to p85α$^{-/-}$ BALB/c mice resulted in increased footpad swelling and animals were no longer able to control the infection. These results

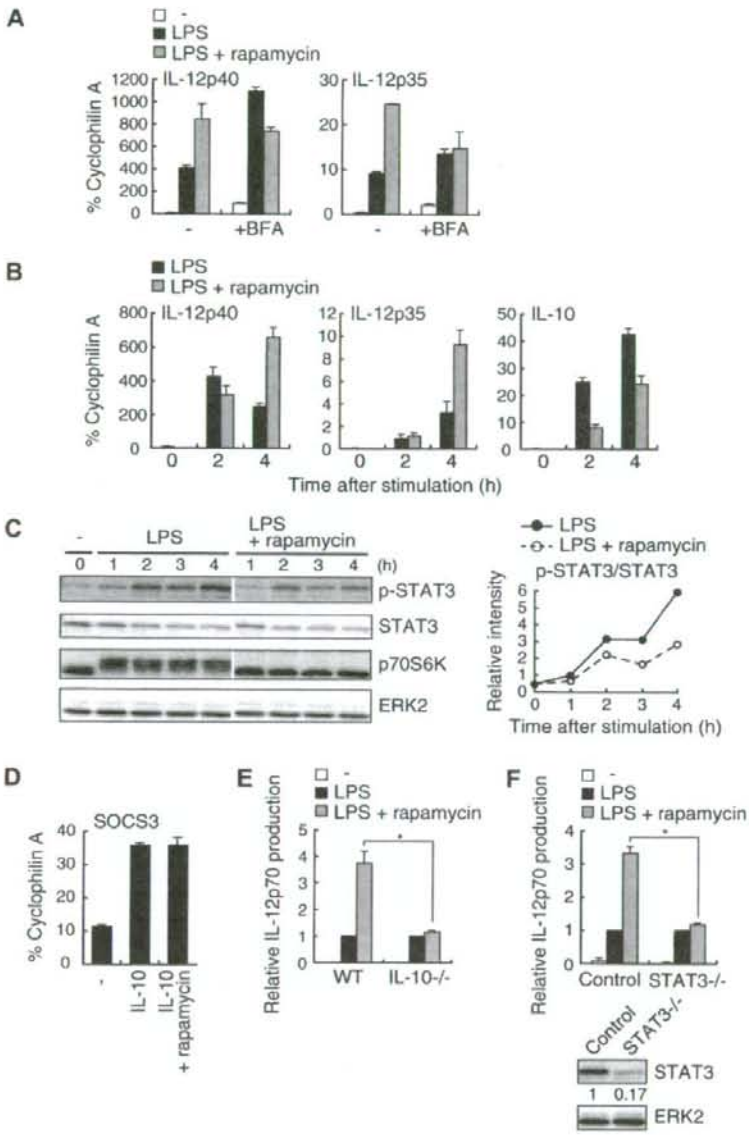

Figure 5. The effect of rapamycin on LPS-induced IL-12 production depends on the IL-10–STAT3 signaling pathway. (A) BMDCs were pretreated with or without 10 ng/mL rapamycin along with or without 5 μg/mL BFA for 20 minutes before stimulation with 1 μg/mL LPS. After 4 hours, total RNA was isolated, and IL-12p40 and IL-12p35 mRNA levels were assessed by real-time PCR using cyclophilin A mRNA as a reference. (B) BMDCs were pretreated with or without 10 ng/mL rapamycin for 20 minutes and then stimulated with 1 μg/mL LPS for the indicated times. Total RNA was isolated, and IL-12p40, IL-12p35, and IL-10 mRNA levels were assessed by real-time PCR using cyclophilin A mRNA as a reference. (C) BMDCs were pretreated with or without 100 ng/mL rapamycin for 20 minutes and then stimulated with 1 μg/mL LPS for the indicated times. The cell lysates were analyzed for phospho-STAT3, STAT3, p70S6K, and ERK2 by Western blotting. The white lines indicate that intervening lanes have been removed. The right panel indicates relative intensities of tyrosine-phosphorylated STAT3 normalized by STAT3 signals. (D) BMDCs were pretreated with or without 100 ng/mL rapamycin for 20 minutes before stimulation with 10 ng/mL IL-10. After 1 hour, total RNA was isolated, and SOCS3 mRNA levels were assessed by real-time PCR using cyclophilin A mRNA as a reference. In panels A, B, and D, data are indicated as mean plus or minus SD of duplicate samples. Data are representative of 2 (B,C) or 3 (A,D) independent experiments with similar results. (E) BMDCs from WT or IL-10$^{-/-}$ mice were stimulated with 1 μg/mL LPS in the presence or absence of 10 ng/mL rapamycin for 24 hours and assayed for the production of IL-12p70 by ELISA. Absolute IL-12p70 levels in the stimulation of LPS alone: WT, 24.1 plus or minus 3.6 pg/mL; IL-10$^{-/-}$, 1120 plus or minus 230 pg/mL. Data are indicated as median plus or minus SD of 3 independent experiments. *$P < .05$ by Mann-Whitney U test comparing WT with IL-10$^{-/-}$ groups. (F) BMDCs from STAT3$^{-/-}$ mice or littermate controls were stimulated with 0.1 μg/mL LPS in the presence or absence of 100 ng/mL rapamycin for 24 hours. Cytokine production was evaluated as in panel E. Absolute IL-12p70 levels in the stimulation of LPS alone: control, 11.8 plus or minus 3.7 pg/mL; STAT3$^{-/-}$, 299 plus or minus 67 pg/mL. *$P < .05$ by Mann-Whitney U test comparing control with STAT3$^{-/-}$ groups. Indicated below are the expression levels of STAT3 and ERK2 in BMDCs determined by Western blotting.

collectively indicate that the attenuation of mTOR and GSK3 by inhibitors affects the balance between Th1 and Th2 responses.

Discussion

We have previously shown that PI3K negatively regulates TLR-induced pro-inflammatory cytokine production by DCs and gut epithelial cells.[8,9,25] Because LPS-induced IL-12 production was decreased in PTEN$^{-/-}$ BMDCs (Figure 1B), the PI3K-Akt pathway triggered by the lipid product of PI3K is indeed important for the suppression of LPS-induced IL-12 production.

Furthermore, our results show that the PI3K-Akt pathway positively regulates IL-10 production. IL-10 is produced by various cell types and plays anti-inflammatory roles in many immune responses.[32] In particular, it has been shown that DC-derived IL-10 is involved in a variety of responses, such as infectious diseases,[33] the induction of tolerance,[34] and cytotoxic T-lymphocyte–mediated antitumor activity.[32] Considering that IL-10 plays a pivotal role in immune regulation, the elucidation of the molecular mechanism underlying PI3K-mediated IL-10 regulation would shed new light on therapeutic approaches toward cancer as well as autoimmune diseases.

Indeed, signaling molecules involved in the PI3K pathway (ie, mTOR and GSK3) seem reasonable targets for appropriately modulating the Th1/Th2 balance. As shown here, the treatment of DCs with rapamycin augments a Th1 response (Figure 7A). Because rapamycin does not alter antigen uptake

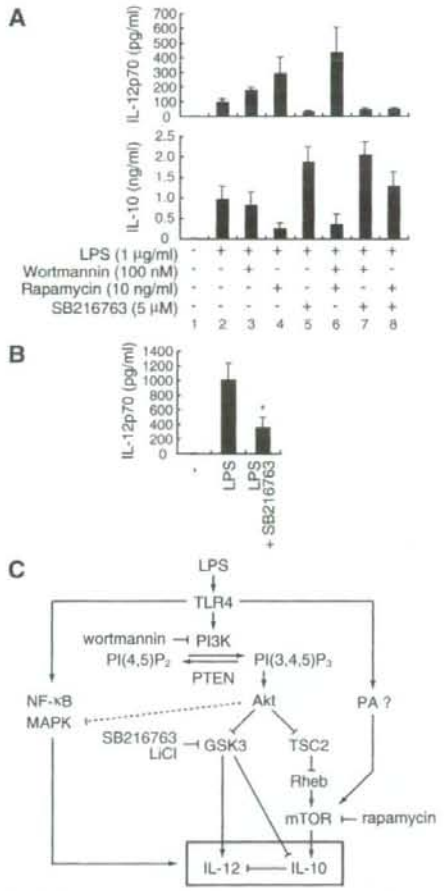

Figure 6. mTOR and GSK3β regulate LPS-induced IL-12 production through distinct mechanisms. (A) BMDCs were stimulated with 1 μg/mL LPS together with the indicated inhibitors for 24 hours and assayed for the production of IL-12p70 and IL-10 by ELISA. Data are indicated as median plus or minus SD of 3 independent experiments. (B) BMDCs from IL-10$^{-/-}$ mice were stimulated with 1 μg/mL LPS in the presence or absence of 5 μM SB216763 for 24 hours and assayed for the production of IL-12p70 by ELISA. Data are indicated as median plus or minus SD of 5 independent experiments. *$P < .05$ by Wilcoxon t test compared with LPS alone. (C) The schematic diagram of the PI3K-mediated regulation of IL-12 production. PA indicates phosphatidic acid; PI(4,5)P_2, phosphatidylinositol(4,5)bisphosphate; PI(3,4,5)P_3, phosphatidylinositol(3,4,5)trisphosphate.

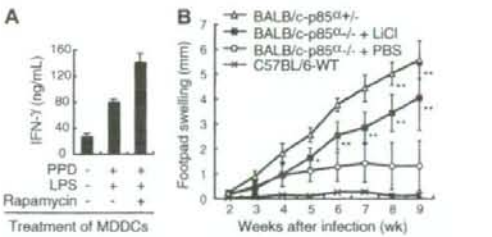

Figure 7. The attenuation of mTOR and GSK3 affects Th1/Th2 balance. (A) Human MDDCs were pretreated with PPD and LPS with or without rapamycin. CD4$^+$ T cells from the same donor were cultured with those MDDCs in the absence of rapamycin. After 1 week of incubation, CD4$^+$ T cells were stimulated with anti-CD3ε and anti-CD28 mAbs for 48 hours and assayed for the production of IFN-γ by ELISA. Data are indicated as median plus or minus SD of duplicate samples. (B) The footpad swelling of *L major*–infected BALB/c-p85α$^{+/-}$ mice treated with LiCl ($n = 8$) or with PBS ($n = 6$) was monitored on a weekly basis. BALB/c-p85α$^{+/-}$ mice ($n = 5$) or C57BL/6-WT mice ($n = 2$) were used as positive and negative controls for *L major* infection, respectively. Data are indicated as median plus or minus SD. *$P < .05$, **$P < .01$ by Mann-Whitney U test compared with PBS-treated BALB/c-p85α$^{+/-}$ mice. There was no significant difference in footpad swelling between LiCl-treated BALB/c-p85α$^{-/-}$ mice and untreated BALB/c-p85α$^{+/-}$ mice.

and presentation,[35] or the expression level of costimulatory molecules such as CD80 and CD86 in DCs,[36] the enhancement of a Th1 response by rapamycin is probably the result of the augmentation of IL-12 production. In addition, the inhibition of GSK3 by LiCl suppressed a Th1-mediated immune response against *L major* in vivo (Figure 7B). These results raise the possibility that the attenuation of these signaling pathways may provide new therapeutic approaches for human diseases.

Based on our present studies as well as other reports, we propose that signal transduction pathways downstream of Akt regulating IL-12 production are composed of at least 3 components: mTOR, GSK3, and MAPK (Figure 6C). First, the mTOR pathway negatively regulates IL-12 production through the induction of IL-10 gene expression. Wortmannin did not completely inhibit the LPS-induced phosphorylation of p70S6K (Figure 2), and a combination of wortmannin and rapamycin further enhanced LPS-induced IL-12 production (Figure 6A), suggesting that the LPS-induced mTOR activation depends only partially on the PI3K pathway. It should be noted that phosphatidic acid produced by LPS stimulation in macrophages activates mTOR in a PI3K-independent manner[37] (Figure 6C).

Second, the GSK3 pathway positively regulates IL-12 production in a more direct manner. Using human monocytes, Martin et al[30] showed that GSK3 positively regulates LPS-induced IL-12p40 production. GSK3 augments the binding of NF-κB p65 to a coactivator "cAMP response element-binding protein" (CREB)-binding protein by competitively inhibiting the binding of CREB to CREB-binding protein.[30] Rodionova et al[31] have also shown that GSK3 enhances IL-12p70 and IL-12p40 production by human *Escherichia coli*–activated MDDCs. Considering that the GSK3-mediated regulation of IL-12 production was independent of IL-10 (Figure 6B), it is probable that GSK3 controls LPS-induced IL-12 production by a mechanism distinct from mTOR.

Third and finally, we and others have reported that the treatment of monocytes or DCs with SB203580, a specific inhibitor of p38, suppressed LPS-induced IL-12 production.[8,11,38] In addition, consistent with the fact that Akt negatively regulates p38,[39] the inhibition of PI3K during LPS activation enhanced p38 phosphorylation and activation[8,24,25] (Figure 2). Conversely, p38 phosphorylation on LPS stimulation was decreased in macrophages derived from PTEN$^{-/-}$ mice.[40] These observations suggest that the PI3K-mediated suppression of p38 results in the attenuation of IL-12 production as well. It has also been reported that the PI3K-Akt pathway negatively regulates JNK activity.[41] Indeed, the treatment of BMDCs with wortmannin slightly enhanced LPS-induced JNK phosphorylation (Figure 2). Studies regarding the function of JNK in LPS-induced IL-12 production using human monocyte cell lines are controversial,[42,43] and the role of JNK in LPS-induced IL-12 production should be evaluated in primary cells, such as BMDCs derived from JNK-deficient mice. Given that rapamycin (Figure 2) and SB216763 (data not shown) had no effect on LPS-induced phosphorylation of p38 and JNK, it seems improbable that mTOR or GSK3 is involved in the PI3K-Akt pathway-mediated negative regulation of p38 and JNK activity. These results taken together indicate that mTOR, GSK3, and MAPK cooperatively regulate TLR-induced IL-12 production in DCs (Figure 6C).

In contrast to IL-10, IFN-β enhances IL-12 production in an autocrine manner.[44] Because wortmannin augments the expression of IFN-β in response to LPS (Figure 3C), it is possible that wortmannin enhances IL-12 production through IFN-β. However, whereas wortmannin enhances the expression of both IL-12p40 and IL-12p35, IFN-β enhances the expression of IL-12p35 but not IL-12p40,[44] suggesting that the effect of wortmannin is probably not mediated by IFN-β. In contrast to wortmannin, rapamycin affected only IL-10 but not IFN-β gene expression (Figure 3C).

Because IL-10 inhibits the LPS-induced production of a diverse array of cytokines, such as IL-6 and TNF-α in addition to IL-12,[28] rapamycin may influence the production of these cytokines. However, we found that rapamycin had no effect on LPS-induced IL-6 and TNF-α production (Figure 3A), consistent with a previous observation that the LPS-induced mRNA expression of IL-12p40, but not TNF-α, is decreased in BMDCs expressing a constitutively active STAT3.[45] Although not shown, rapamycin also augmented IL-12p40 production and suppressed IL-10 production in mouse BMDCs in response to other TLR ligands, such as zymosan (for TLR2/6) and CpG-ODN (for TLR9), whereas it had no effect on IL-6 production. It is possible that the expression of those cytokines has different sensitivities to the negative regulation by IL-10.

What is the molecular mechanism underlying the PI3K-mediated regulation of LPS-induced IL-10 production? p70S6K, one of the targets regulated by mTOR, is able to increase the translation of a subset of mRNAs that contain a 5′ tract of oligopyrimidine.[46] However, the 5′ tract of oligopyrimidine was not detected in mouse or human IL-10 mRNA. Another target molecule, 4E-BP1, regulates eIF-4E, which stimulates translational initiation but whose function is thought to be general and not restricted to a subset of genes. mTOR is also involved in gene transcription through the regulation of transcriptional factors without a translational event.[14,47,48] This mechanism is more probable because our observations indicate that rapamycin suppresses LPS-induced IL-10 production at a transcriptional level (Figure 3C), rather than through translational regulators. However, the DNA binding of transcriptional factor Sp1 to the *IL10* promoter in LPS-stimulated mice BMDCs was unaffected in the presence of rapamycin (data not shown). The regulation by transcription factors downstream of mTOR remains to be elucidated in future studies. In addition to mTOR, GSK3 is involved in a regulatory pathway for IL-10 production. Indeed, GSK3 negatively regulated LPS-induced IL-10 production (Figure 6A), presumably by inactivation of CREB,[30] which is involved in the transcriptional activation of the *IL10* gene.

It should be noted that many previous studies on the regulation of IL-10 or IL-12 gene expression were performed using macrophage or DC cell lines. We have been aware that cell lines and primary cells often showed different results. One obvious problem is the fact that many cell lines have some defect or alteration in PI3K-PTEN regulation, such that many immortalized cell lines lack PTEN expression and show enhanced Akt activity. These cells are obviously not suitable for studying PI3K pathways. Detailed analysis with primary cells is important in future studies.

Acknowledgments

The authors thank Drs A. Suzuki, H. Miyoshi, and K. Takeda for valuable materials, Dr T. Luft of German Cancer Research Center for valuable discussion and sharing unpublished data, and Dr Linda K. Clayton of Harvard Medical School for critically reading the manuscript.

This work was supported by the Uehara Memorial Foundation, a Keio Gijuku Academic Development Fund (S. Matsuda), a Grant-in-Aid for Scientific Research (C 19590499; S. Matsuda) from the Japan Society for the Promotion of Science, a Grant-in-Aid for Scientific Research on Priority Areas (14021110 and 18073015), a National Grant-in-Aid for the Establishment of a High-Tech Research Center in a private university, and a Scientific Frontier Research Grant from the Ministry of Education, Culture, Sports, Science and Technology, Japan.

Authorship

Contribution: M.O. designed the research, performed experiments, and wrote the paper; S.N., S. Kondo, S. Mizuno, K.N., and M.T. performed experiments; T.T. and S. Matsuda designed the research; and S. Koyasu designed the research and wrote the paper.

Conflict-of-interest disclosure: The authors declare no competing financial interests.

Correspondence: Shigeo Koyasu, Department of Microbiology and Immunology, Keio University School of Medicine, 35 Shinanomachi, Shinjuku-ku, Tokyo 160-8582, Japan; e-mail: koyasu@sc.itc.keio.ac.jp.

References

1. Banchereau J, Briere F, Caux C, et al. Immunobiology of dendritic cells. Annu Rev Immunol. 2000; 18:767-811.
2. Steinman RM, Hemmi H. Dendritic cells: translating innate to adaptive immunity. Curr Top Microbiol Immunol. 2006;311:17-58.
3. Takeda K, Kaisho T, Akira S. Toll-like receptors. Annu Rev Immunol. 2003;21:335-376.
4. Creagh EM, O'Neill LA. TLRs, NLRs and RLRs: a trinity of pathogen sensors that co-operate in innate immunity. Trends Immunol. 2006;27:352-357.
5. Trinchieri G. Interleukin-12 and the regulation of innate resistance and adaptive immunity. Nat Rev Immunol. 2003;3:133-146.
6. Vanhaesebroeck B, Leevers SJ, Ahmadi K, et al. Synthesis and function of 3-phosphorylated inositol lipids. Annu Rev Biochem. 2001;70:535-602.
7. Koyasu S. The role of PI3K in immune cells. Nat Immunol. 2003;4:313-319.
8. Fukao T, Tanabe M, Terauchi Y, et al. PI3K-mediated negative feedback regulation of IL-12 production in DCs. Nat Immunol. 2002;3:875-881.
9. Fukao T, Koyasu S. PI3K and negative regulation of TLR signaling. Trends Immunol. 2003;24:358-363.
10. Fukao T, Yamada T, Tanabe M, et al. Selective loss of gastrointestinal mast cells and impaired immunity in PI3K-deficient mice. Nat Immunol. 2002;3:295-304.
11. Goodridge HS, Harnett W, Liew FY, Harnett MM. Differential regulation of interleukin-12 p40 and p35 induction via Erk mitogen-activated protein kinase-dependent and -independent mechanisms and the implications for bioactive IL-12 and IL-23 responses. Immunology. 2003;109:415-425.
12. Martin M, Schifferle RE, Cuesta N, Vogel SN, Katz J, Michalek SM. Role of the phosphatidylinositol 3 kinase-Akt pathway in the regulation of IL-10 and IL-12 by Porphyromonas gingivalis lipopolysaccharide. J Immunol. 2003;171:717-725.
13. Kuo CC, Lin WT, Liang CM, Liang SM. Class I and III phosphatidylinositol 3′-kinase play distinct roles in TLR signaling pathway. J Immunol. 2006; 176:5943-5949.
14. Wullschleger S, Loewith R, Hall MN. TOR signaling in growth and metabolism. Cell. 2006;124: 471-484.
15. Suzuki H, Terauchi Y, Fujiwara M, et al. Xid-like immunodeficiency in mice with disruption of the p85alpha subunit of phosphoinositide 3-kinase. Science. 1999;283:390-392.
16. Terauchi Y, Tsuji Y, Satoh S, et al. Increased insulin sensitivity and hypoglycaemia in mice lacking the p85 alpha subunit of phosphoinositide 3-kinase. Nat Genet. 1999;21:230-235.
17. Takeda K, Clausen BE, Kaisho T, et al. Enhanced Th1 activity and development of chronic enterocolitis in mice devoid of Stat3 in macrophages and neutrophils. Immunity. 1999; 10:39-49.
18. Clausen BE, Burkhardt C, Reith W, Renkawitz R,

Forster I. Conditional gene targeting in macrophages and granulocytes using LysMcre mice. Transgenic Res. 1999;8:265-277.

19. Suzuki A, Yamaguchi MT, Ohteki T, et al. T cell-specific loss of Pten leads to defects in central and peripheral tolerance. Immunity. 2001;14:523-534.
20. Miyoshi H, Blomer U, Takahashi M, Gage FH, Verma IM. Development of a self-inactivating lentivirus vector. J Virol. 1998;72:8150-8157.
21. Nagai T, Ibata K, Park ES, Kubota M, Mikoshiba K, Miyawaki A. A variant of yellow fluorescent protein with fast and efficient maturation for cell-biological applications. Nat Biotechnol. 2002;20:87-90.
22. Suzue K, Kobayashi S, Takeuchi T, Suzuki M, Koyasu S. Critical role of dendritic cells in determining the Th1/Th2 balance and the disease outcome upon *Leishmania major* infection. Int Immunol. 2008;20:337-343.
23. Cross DA, Alessi DR, Cohen P, Andjelkovich M, Hemmings BA. Inhibition of glycogen synthase kinase-3 by insulin mediated by protein kinase B. Nature. 1995;378:785-789.
24. Guha M, Mackman N. The phosphatidylinositol 3-kinase-Akt pathway limits lipopolysaccharide activation of signaling pathways and expression of inflammatory mediators in human monocytic cells. J Biol Chem. 2002;277:32124-32132.
25. Yu Y, Nagai S, Wu H, Neish AS, Koyasu S, Gewirtz AT. TLR5-mediated phosphoinositide 3-kinase activation negatively regulates flagellin-induced proinflammatory gene expression. J Immunol. 2006;176:6194-6201.
26. Bierer BE, Mattila PS, Standaert RF, et al. Two distinct signal transmission pathways in T lymphocytes are inhibited by complexes formed between an immunophilin and either FK506 or rapamycin. Proc Natl Acad Sci U S A. 1990;87:9231-9235.
27. Long X, Lin Y, Ortiz-Vega S, Yonezawa K, Avruch J. Rheb binds and regulates the mTOR kinase. Curr Biol. 2005;15:702-713.
28. Moore KW, de Waal Malefyt R, Coffman RL, O'Garra A. Interleukin-10 and the interleukin-10 receptor. Annu Rev Immunol. 2001;19:683-765.
29. Ding Y, Chen D, Tarcsafalvi A, Su R, Qin L, Bromberg JS. Suppressor of cytokine signaling 1 inhibits IL-10-mediated immune responses. J Immunol. 2003;170:1383-1391.
30. Martin M, Rehani K, Jope RS, Michalek SM. Toll-like receptor-mediated cytokine production is differentially regulated by glycogen synthase kinase 3. Nat Immunol. 2005;6:777-784.
31. Rodionova E, Conzelmann M, Maraskovsky E, et al. GSK-3 mediates differentiation and activation of proinflammatory dendritic cells. Blood. 2007; 109:1584-1592.
32. Mocellin S, Marincola FM, Young HA. Interleukin-10 and the immune response against cancer: a counterpoint. J Leukoc Biol. 2005;78:1043-1051.
33. McGuirk P, McCann C, Mills KH. Pathogen-specific T regulatory 1 cells induced in the respiratory tract by a bacterial molecule that stimulates interleukin 10 production by dendritic cells: a novel strategy for evasion of protective T helper type 1 responses by Bordetella pertussis. J Exp Med. 2002;195:221-231.
34. Akbari O, DeKruyff RH, Umetsu DT. Pulmonary dendritic cells producing IL-10 mediate tolerance induced by respiratory exposure to antigen. Nat Immunol. 2001;2:725-731.
35. Lee YR, Yang IH, Lee YH, et al. Cyclosporin A and tacrolimus, but not rapamycin, inhibit MHC-restricted antigen presentation pathways in dendritic cells. Blood. 2005;105:3951-3955.
36. Hackstein H, Taner T, Zahorchak AF, et al. Rapamycin inhibits IL-4-induced dendritic cell maturation in vitro and dendritic cell mobilization and function in vivo. Blood. 2003;101:4457-4463.
37. Foster DA. Regulation of mTOR by phosphatidic acid? Cancer Res. 2007;67:1-4.
38. Puig-Kroger A, Relloso M, Fernandez-Capetillo O, et al. Extracellular signal-regulated protein kinase signaling pathway negatively regulates the phenotypic and functional maturation of monocyte-derived human dendritic cells. Blood. 2001; 98:2175-2182.
39. Kim AH, Khursigara G, Sun X, Franke TF, Chao MV. Akt phosphorylates and negatively regulates apoptosis signal-regulating kinase 1. Mol Cell Biol. 2001;21:893-901.
40. Cao X, Wei G, Fang H, et al. The inositol 3-phosphatase PTEN negatively regulates Fc gamma receptor signaling, but supports Toll-like receptor 4 signaling in murine peritoneal macrophages. J Immunol. 2004;172:4851-4857.
41. Park HS, Kim MS, Huh SH, et al. Akt (protein kinase B) negatively regulates SEK1 by means of protein phosphorylation. J Biol Chem. 2002;277: 2573-2578.
42. Utsugi M, Dobashi K, Ishizuka T, et al. c-Jun N-terminal kinase negatively regulates lipopolysaccharide-induced IL-12 production in human macrophages: role of mitogen-activated protein kinase in glutathione redox regulation of IL-12 production. J Immunol. 2003;171:628-635.
43. Ma W, Gee K, Lim W, et al. Dexamethasone inhibits IL-12p40 production in lipopolysaccharide-stimulated human monocytic cells by down-regulating the activity of c-Jun N-terminal kinase, the activation protein-1, and NF-kappa B transcription factors. J Immunol. 2004;172:318-330.
44. Gautier G, Humbert M, Deauvieau F, et al. A type I interferon autocrine-paracrine loop is involved in Toll-like receptor-induced interleukin-12p70 secretion by dendritic cells. J Exp Med. 2005;201: 1435-1446.
45. Hoentjen F, Sartor RB, Ozaki M, Jobin C. STAT3 regulates NF-κB recruitment to the IL-12p40 promoter in dendritic cells. Blood. 2005;105: 689-696.
46. Jefferies HB, Fumagalli S, Dennis PB, Reinhard C, Pearson RB, Thomas G. Rapamycin suppresses 5'TOP mRNA translation through inhibition of p70s6k. EMBO J. 1997;16:3693-3704.
47. Soliman GA. The mammalian target of rapamycin signaling network and gene regulation. Curr Opin Lipidol. 2005;16:317-323.
48. Cunningham JT, Rodgers JT, Arlow DH, Vazquez F, Mootha VK, Puigserver P. mTOR controls mitochondrial oxidative function through a YY1-PGC-1alpha transcriptional complex. Nature. 2007; 450:736-740.

Automated Microfluidic Assay System for Autoantibodies Found in Autoimmune Diseases Using a Photoimmobilized Autoantigen Microarray

Takahiro Matsudaira
Nano Medical Enginering Laboratory, RIKEN (The Institute of Physical and Chemical Research), Wako, Saitama, Japan

Saki Tsuzuki
Regenerative Medical Bioreactor Project, Kanagawa Academy of Science and Technology, Takatsu-Ku, Kawasaki, Kanagawa, Japan

Akira Wada
Nano Medical Enginering Laboratory, RIKEN (The Institute of Physical and Chemical Research), Wako, Saitama, Japan

Akira Suwa
School of Medicine, Tokai University, 143 Shimokasuya, Isehara, Kanagawa, Japan

Hitoshi Kohsaka
Dept. of Medicine and Rheumatology, Graduate School, Tokyo Medical and Dental University, Bunkyo-ku, Tokyo, Japan

Maiko Tomida
Moritex Co. 1-3-3 Azamino-Minami, Aoba-ku, Yokohama, Kanagawa, Japan

Yoshihiro Ito
Nano Medical Enginering Laboratory, RIKEN (The Institute of Physical and Chemical Research), Wako, Saitama, Japan

Regenerative Medical Bioreactor Project, Kanagawa Academy of Science and Technology, Takatsu-Ku, Kawasaki, Kanagawa, Japan

DOI 10.1021/bp.63
Published online November 24, 2008 in Wiley InterScience (www.interscience.wiley.com).

Autoimmune diseases such as rheumatoid arthritis, multiple sclerosis, and autoimmune diabetes are characterized by the production of autoantibodies that serve as useful diagnostic markers, surrogate markers, and prognostic factors. We devised an in vitro system to detect these clinically pivotal autoantibodies using a photoimmobilized autoantigen microarray. Photoimmobilization was useful for preparing the autoantigen microarray, where autoantigens are covalently immobilized on a plate, because it does not require specific functional groups of the autoantigens and any organic material can be immobilized by a radical reaction induced by photoirradiation. Here, we prepared the microarray using a very convenient method. Aqueous solutions of each autoantigen were mixed with a polymer of poly(ethylene glycol) methacrylate and a photoreactive crosslinker, and the mixtures were microspotted on a plate and dried in air. Finally, the plate was irradiated with an ultraviolet lamp to obtain immobilization. In the assay, patient serum was added to the microarray plate. Antigen-specific IgG adsorbed on the microspotted autoantigen was detected by peroxidase-conjugated anti-IgG antibody. The chemical luminescence intensities of the substrate decomposed by the peroxidase were detected with a sensitive CCD camera. All autoantigens were immobilized stably by this method and used to screen antigen-specific IgG. In addition, the plate was covered with a polydimethylsiloxane sheet containing microchannels and automated measurement was carried out.
Keywords: antigen microarray, autoimmune disease diagnosis, chemiluminescence, photoimmobilization, automation, microfluid

Introduction

Autoimmune diseases affect an estimated 3–5% of the total population.[1,2] Many of them are characterized by the presence of autoantibodies, and the pattern of antibodies present is used to distinguish disorders in this group.[3] Common laboratory methods for detecting antibodies in serum include indirect immunofluorescence microscopy, enzyme-linked immunosorbent assays (ELISA), and immunoblot assays.[4] Indirect immunofluorescence microscopy traditionally uses carcinoma cell lines in reactions with

Correspondence concerning this article should be addressed to Y. Ito at y-ito@riken.jp.

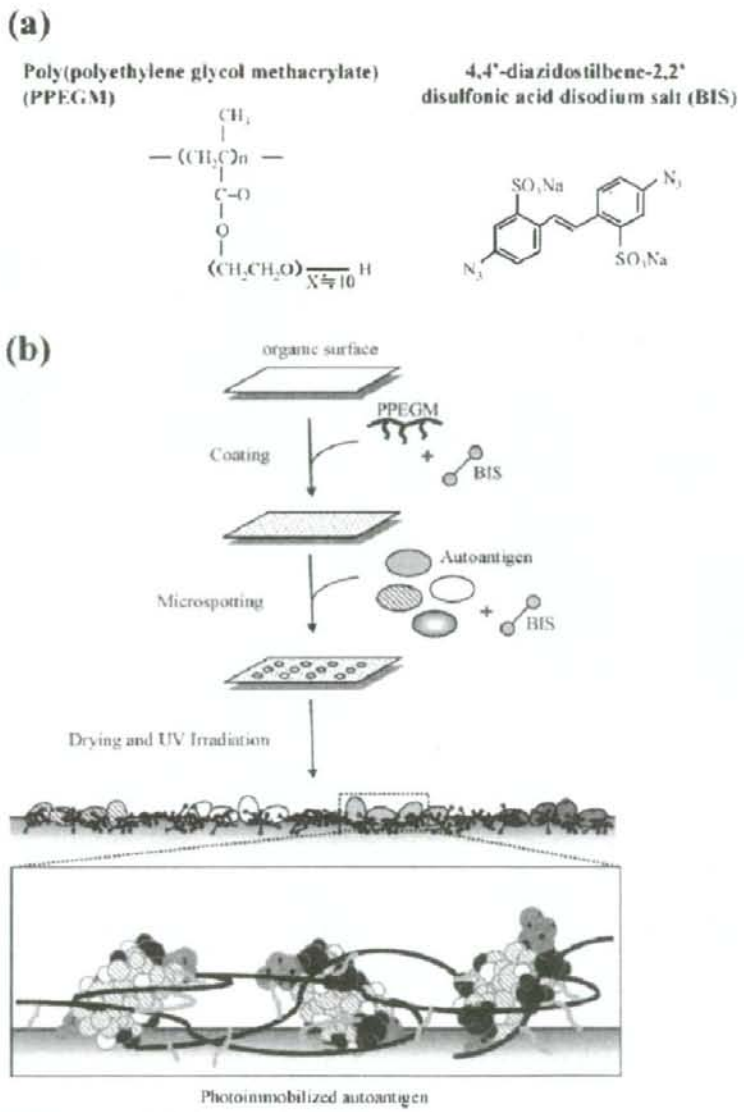

Figure 1. (a) Chemical structures and (b) illustration of the photoimmobilization.

Abbreviations: PPEGM, polymer carrying polyethylene glycol in the side chains; BIS, 4,4'-diazidostilbene-2,2'-disulfonic acid disodium salt.

serum samples. A major drawback of this approach is that it does not define the specific antigen and thus is unable to provide information for the design of specific treatment strategies. Advances in molecular biology have contributed to the identification of autoantigens and allowed their production, thus making assays for them feasible. However, until now, each autoantibody has been determined by a separate assay and results from different assay systems are not interchangeable.[5]

In recent years, biochip/microarray technology has become a powerful tool for parallel analysis.[6] In addition to nucleic acid-based arrays, various types of microarray systems have been developed.[7-11] Among these systems, antigen and allergen microarrays have been reported by several researchers.[12-31] In addition, autoantigen microarrays have been investigated.[32-40] However, because the immobilization techniques were based either on physical adsorption of antigens or covalent bonding of amino groups in the antigens, it was

possible that some antigens were not immobilized or not stably immobilized. Therefore, a new immobilization method using photoirradiation has been devised and used in the preparation of microarrays by several researchers.[41-55] The advantages of the photoimmobilization method are that it is not limited by functional groups and that it can immobilize any organic material in any organic substrate. In addition, as a result of the lack of a requirement for functional groups, the orientation of the photoimmobilized macromolecules is random, leaving various sites exposed for interaction with polyclonal antibodies. This is also important for monoclonal antibodies, where the necessary orientation is not known or controllable.

We have developed a new photoimmobilization method incorporating a nonbiofouling polymer, polyethylene glycol.[31,41-44] In particular, a polymer carrying polyethylene glycol in the side chains poly(polyethylene glycol methacrylate) (PPEGM), which is a vinyl polymer containing polyethylene glycol (PEG) brush, has been employed in previous studies, and it was demonstrated that PPEGM was more effective for antibiofouling than the usual PEG.[31,41] By this method, nonspecific interaction was reduced, and various types of molecules were easily immobilized in the microarray by the same method. In addition, our photoimmobilization method is very convenient because the system consists only of a mixture of matrix polymer and photoreactive crosslinker. In this investigation, we applied the method to immobilization of autoantigens and developed an automated assay system using a microfluidic device.

Materials and Methods

Reagents and sera

Plates (polystyrene, 2.5 cm × 7.6 cm × 0.5 mm) were cleaned using ethanol, with sonication for 15 min at room temperature. Washed polystyrene plates were dried and stored. The autoantigens Ro/SS-A (52 kDa), Ro/SS-A (60 kDa), U1snRNP (68 kDa), U-snRNA B/B', Jo-1, dsDNA, and CENP-B were purchased from Diarect (Freiburg, Germany), SS-B/La and Scl-70 were purchased from Fitzgerald (Massachusetts), and SS-A and Sm were kindly provided by Medical & Biological Laboratories (MBL, Nagoya, Japan). The polyclonal affinity-purified horseradish peroxidase (HRP)-labeled goat anti-human IgG antibody was purchased from GE Healthcare (Oxford, UK) and HRP-labeled sheep anti-human IgM antibody was purchased from Chemicon (Victoria, Australia). The ECL Advance Kit for HRP was purchased from Amersham Biosciences UK Ltd. (Buckinghamshire, UK). 4,4'-Diazido-stylbene-2,2'-disulfonic acid disodium salt (BIS), polyethylene glycol methacrylate (PEGM, molecular weight 350 Da), and bovine serum albumin (BSA) were purchased from Sigma–Aldrich Co (Milwaukee, WI). Human Autoantibody positive sera were purchased from Medical & Biological Laboratories (MBL, Nagoya, Japan).

Autoantibody-positive sera were purchased from MBL. Sera from patients with autoimmune diseases were obtained from the Keio University Hospital with informed consent. Characteristics of autoantibodies were identified in Ouchterlony immunodiffusion, ELISA, immunoblot, and immunoprecipitation assays.

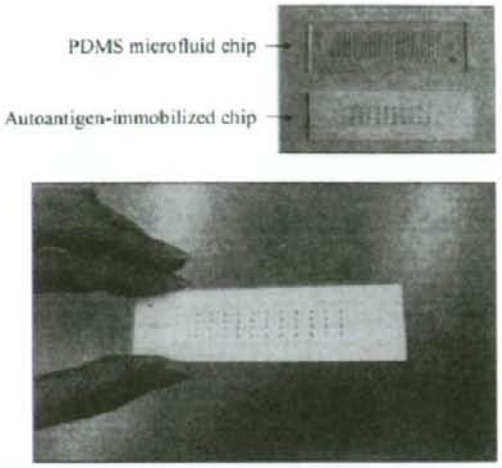

Figure 2. Photographs of a polystyrene chip where dye was microspotted for visualization and a PDMS chip with a microfluid channel.

The two plates were superimposed during the assay.

Synthesis of polymerized PEGM (PPEGM)

The polymer matrix carrying polyethylene glycol in the side chains (PPEGM) was prepared as follows. Polyethylene glycol methacrylate (7.0 g) was dissolved in ethyl acetate (80 mL) and bubbled with nitrogen gas for 30 s. Azobisisobutyronitrile (46.0 mg) was added to the solution, which was then allowed to stand for 6 h at 60°C. The solution was concentrated and added to diethyl ether. A viscous solid was obtained after stirring. The precipitation procedure was repeated four times and the final precipitate was dried *in vacuo*. The yield was 1.57 g (22.4%).

Photoimmobilization of autoantigens

Photoimmobilization was performed as illustrated in Figure 1. An aqueous solution of BIS (2.5 mg/mL), PPEGM (50 mg/mL), and Tween 20 (5%) were mixed in phosphate-buffered solution (PBS) and spin-coated on the plate. Autoantigens (1 mg/mL) were dissolved in deionized water with BIS (0.1 mg/mL), the aqueous solutions were microspotted onto the plate (50 nL) with a microarray spotter (PixSis-4500, Cartesian, Irvine, CA) and the droplets were dried. The microarrayed plate was irradiated with an ultraviolet lamp (300–400 nm, Nippo Electric Co. Ltd FL15BLB, 1.6 mW/cm^2) for 7 min. Finally, the autoantigen-immobilized plates were rinsed with PBS containing 0.1% Tween-20 (the washing buffer) and stored at −20°C until use.

Microarray assay procedure

The serum was diluted 100-fold with PBS. The autoantigen-immobilized plates were incubated with the diluted serum (100μL) in a chamber for 20 min at room temperature, with shaking. The plate was washed with 30 mL of the washing buffer for 3 min in a chamber. HRP-conjugated anti-human-IgG antibody (diluted 1:100 with BSA–saturated PBS) was loaded on the microarray plates, and the plates

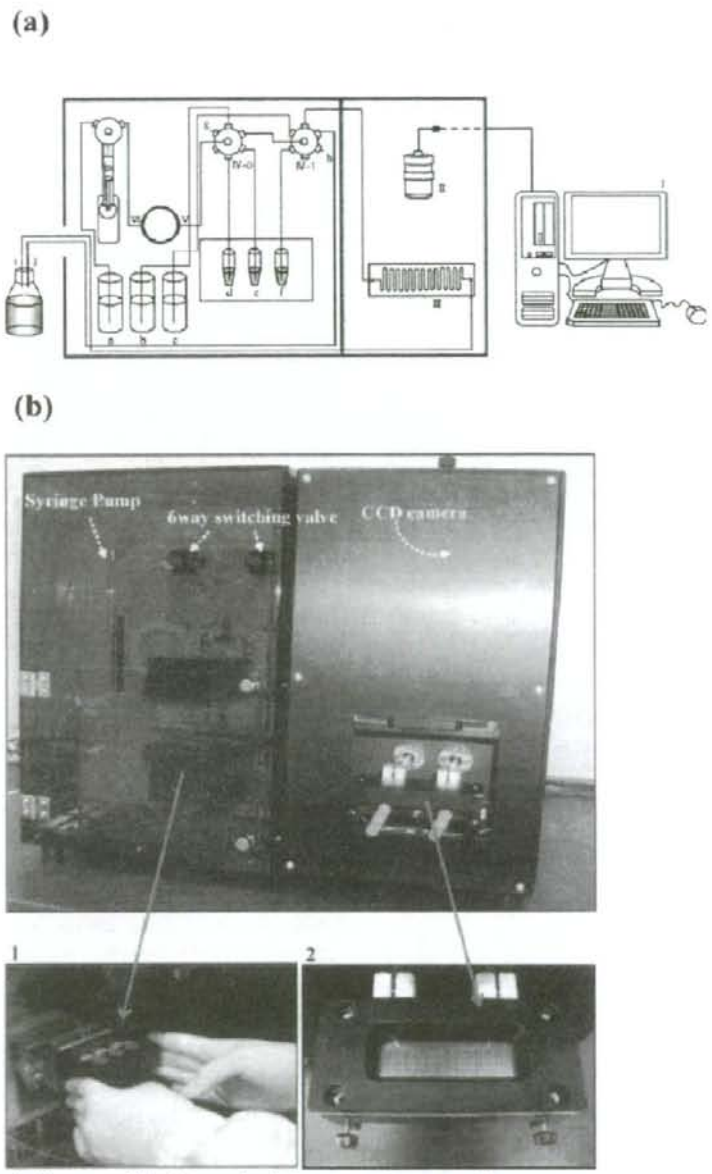

Figure 3. (a) Schematic diagram and (b) photographs of the automated assay machine.

I, personal computer; II, CCD camera; III, cell for sheets described in Figure 2; IV-0 and IV-1, 6-way switching valves; V, sample loop; VI, diluter; a, system solution; b, PBS; c, PBS containing surfactant; d, sample serum; e, secondary antibody; f, chemiluminescence reagent solution; g and h, air; i and j, waste solutions.

were incubated in a chamber for 1 h at room temperature, with shaking. Finally, the substrate solutions (ECL Advance Kit) were added to the plates and incubated for 3 min at room temperature. The chemical luminescence intensity of each microspot was measured for 30 s using a cooled CCD camera system (AE-6960 Light Capture, ATTO Co., Tokyo, Japan).

Conventional assay kits using ELISA were purchased from MBL and used according to the manufacturer's protocol.

Setup of automated assay system

For automated assays, a microfluid plate made of polydimethylsilicone containing a channel (dimensions: width = 1 mm,

depth = 0.5 mm) was prepared and the transparent plate was superimposed on the microspotted polystyrene plate as shown in Figure 2. The setup of the automated assay system is shown in Figure 3. The system consisted of a personal computer, CCD camera (380,000 pixels), syringe pump, and valves (standard micropipette manufactured) to manipulate three processes for flow of samples, HRP-labeled IgG, and chemical luminescence reagents. The tubes containing serum and aqueous solutions of regents were stored in cool places. After the samples and autoantigen-immobilized plate had been placed into the system, the assay was started by switching on the personal computer. Data were automatically collected and displayed on the monitor.

Results

Photoimmobilization

We propose that BIS works as a photoreactive crosslinker to immobilize the autoantigen within PPEGM and that photoirradiation causes crosslinking reactions to occur between autoantigen and PPEGM, autoantigen and the plate surface, and PPEGM and the plate surface.

Autoantibodies adsorbed onto the microspotted autoantigens and could be detected by the chemical luminescence produced by secondary antibodies labeled with horseradish peroxidase (HRP). We compared the effect of photoimmobilization with physical adsorption of autoantigens on an unmodified plate, as shown in Figure 4. It was apparent that the size of the microspotted autoantigens depended significantly on the kind of autoantigen, and that the shapes of the microspots were deformed (not the original circular shape) and different from each other. These results demonstrated that microspotting by physical adsorption cannot be performed stably. In addition, nonspecific adsorption of serum of some patients was observed on the plate and antibodies against dsDNA were not detected, because no immobilization of dsDNA occurred on the plate. Although it was difficult to determine the degree of adsorption or immobilization of the autoantigens in the commercially available ELISA kit, the method was considered to be different from the simple physical adsorption performed in this study. Otherwise, in the case of ELISA, the amount of adsorbed or immobilized autoantigens on the large area of the wells would be so high that it would not affect the assay.

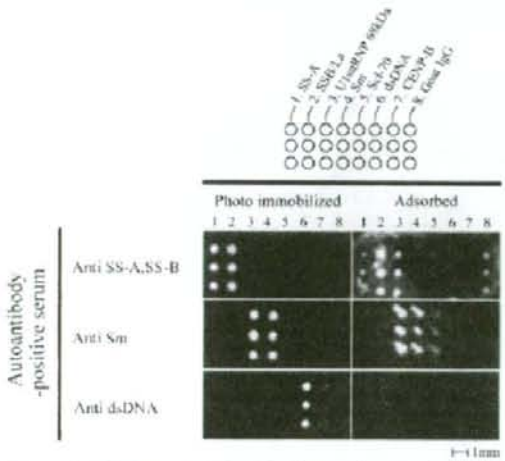

Figure 4. CCD-captured chemiluminescent images of photoimmobilized (left) and physically adsorbed (right) autoantigens after reaction with an autoantibody-positive serum.

Physical adsorption was performed without the crosslinker BIS on the plate after coating with PPEGM and BIS.

Table 1. Correlation Coefficients Between Microarray and Conventional ELISA Assays

Autoantigen	Detected	Correlation Coefficient
SS-A	Anti SS-A antibody	0.94
SS-B/La	Anti SS-B antibody	0.92
U1snRNP68kDa	Anti U1RNP antibody	0.83
Sm	Anti Sm antibody	0.92
Scl-70	Anti Scl-70 antibody	0.97
dsDNA(Plasmid)	Anti dsDNA antibody	0.89
CENP-B	Anti Centromere antibody	0.97
IgG from goat serum	IgM-RF	0.85

On the other hand, the photoimmobilized spot was uniform and stable, and no nonspecific adsorption of serum was observed on the plate, because polyethylene glycol was photoimmobilized. In addition, autoantibodies against dsDNA were detected on photoimmobilized dsDNA because photoimmobilization caused covalent bonding without any requirement of functional groups.

Comparison with conventional assay

In this investigation, the highest intensity in the microspot image was measured and the relationship between this intensity and conventional ELISA results was investigated. Results are shown in Table 1. Strong correlations between conventional ELISA and microarray assays were obtained for every autoantigen.

Specific autoantibodies are present in the most common systemic autoimmune diseases, including mixed connective tissue disease, Sjogren syndrome (SS), system lupus erythematosus, and systemic sclerosis. Figure 5 shows examples of autoantibodies detected by ELISA and images of

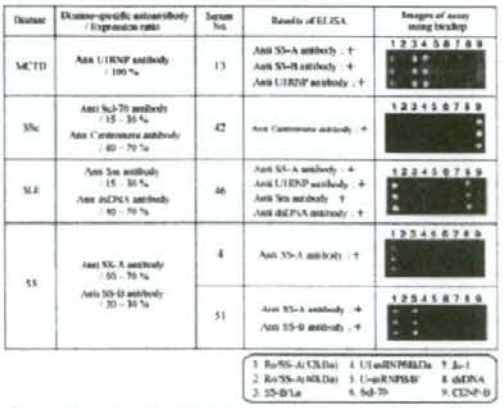

Figure 5. Autoantibody tests requested most frequently for each immune disease and the CCD-captured image of a microarray assay.

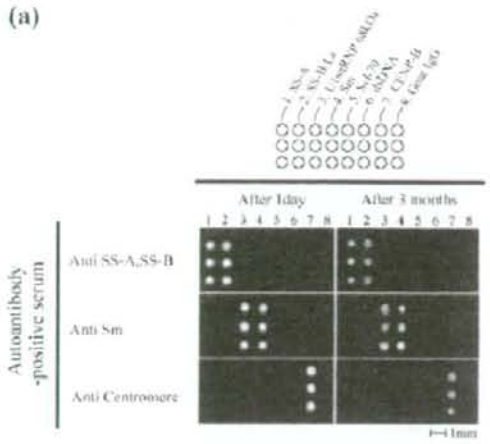

Figure 6. (a) Chemiluminescence image, and (b) comparison of intensity of microarray assays after 1 day and after 3 months.

The correlation coefficients are indicated by *R*.

microarray assays. Because the two assays agreed well, the microarray assay is useful for identifying these marker autoantibodies.

Table 2. Flow Chart of Automated Microarray Assay

	Menu	Time	
1	Default	0	
2	Supplying Ultrapure water	1′ 00″	
3	Supplying PBS	0′ 50″	
4	Supplying Serum	0′ 50″	1 Cycle
5	Serum reaction (1st reaction)	7′ 35″	
6	Washing	1′ 45″	
7	Supplying Enzyme-labeled antibody	0′ 50″	
8	2nd reaction	7′ 35″	
9	Washing	1′ 45″	
10	Supplying chemilumigenic reagent	0′ 55″	
11	Chemiluminescene reaction	7′ 45″	
12	Washing	5′ 45″	
13	Exit operation	15′ 55″	

Stability of the microarray chip

The stability of the microarray chip was examined by comparing assay results after 1 day and 3 months. No significant difference was observed, as shown in Figure 6. The reactivity of photoimmobilized autoantigens remained stable for at least 3 months at −20°C.

Automated microarray assay

Table 2 shows the flow chart of an automated microarray assay. After sample and reagent tubes were attached to holders and the microarray plate was attached to the cell holder, the switch on the personal computer was turned on. The remainder of the process was performed automatically. Washing was performed by two-way movement of flow with both ends capped by gas. The time for each process step was adjusted to minimize the measurement time. In our system, a new serum sample can be assayed automatically about every 30 min.

Figure 7 shows the chemical luminescence image captured by the CCD camera in the automated system. Signal spots could be seen clearly. Figure 8 compares signal intensities between manual and automatic assay methods. Although the photoimmobilized autoantigen was distributed along the fluid path, there was no significant difference along the path

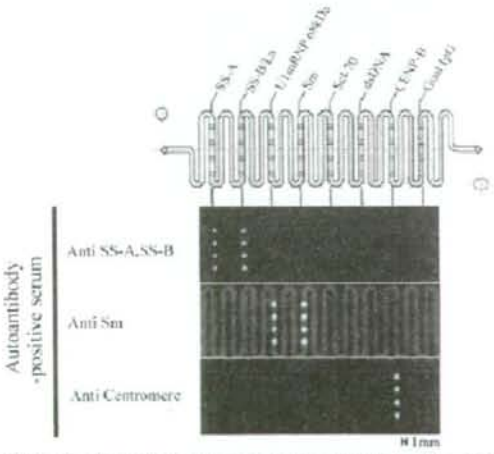

Figure 7. Chemiluminescence images captured by the CCD mounted in the automated assay machine.

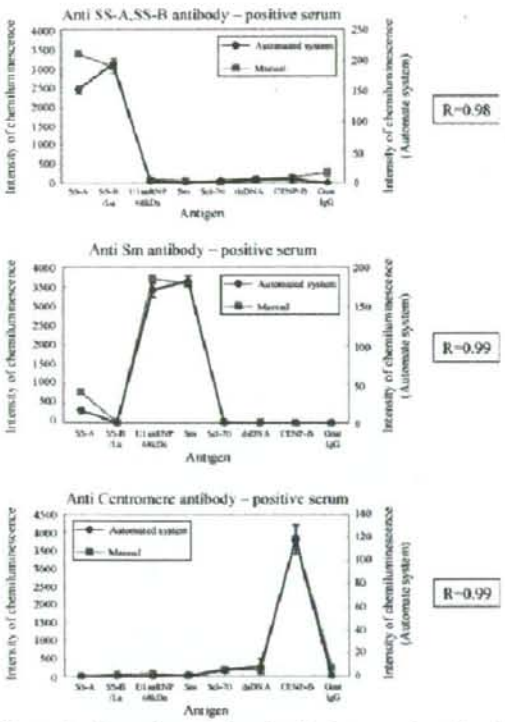

Figure 8. Comparison of the chemiluminescence intensity of image captured by manual and automated CCDs, which were 12 and 8 bit, respectively.

The correlation coefficients are indicated by *R*.

length. It seems that the amount of fluid was sufficient that no significant loss of sample or reagents occurred during flow along the microfluid path.

Discussion

The photoimmobilization method has been used for immobilization or crosslinking of biomolecules for many years. Arylazides, diaziridines, benzophenones, and nitrobenziles, which are activated by irradiation at wavelengths greater than 350 nm (where most biomolecules are transparent), have been used. It is known that arylazide is activated via photolysis, resulting in reactive nitrene, which can insert C—H bonds. However, nitrene intermediates undergo rapid intramolecular ring expansion reactions leading to highly electrophilic cyclic compounds, which exhibit a relatively slow insertion rate. The undesired ring expansion reaction can be minimized by using perfluorophenylazides with fluorine substituents on aromatic rings, but nonfluorinated arylazides work. The photoimmobilization method enables immobilization of any organic material, independently of functional groups or proteins.[45–56]

In this study, to simplify the method, we used a commercially available photocrosslinker, BIS. By this method, we could conveniently prepare multiple microspots according to the same method. Although dsDNA was not immobilized by physical adsorption, the photoimmobilization method enabled stable immobilization. This is because photoimmobilization requires no functional groups, but instead produces covalent bonding.

The second advantage of the photoimmobilization is that the orientation of immobilized molecules is random. This property is suitable for the assay of polyclonal antibodies because various sites of immobilized molecules are exposed at the surface (Fig. 1). It is also this property that makes it possible to determine IgG in small areas with the same linearity as the standard ELISA.

The third advantage of photoimmobilization is reduction of nonspecific adsorption of serum proteins that interrupt the signals from autoantigen-specific IgGs. The polyethylene glycol polymer used in this study efficiently reduced nonspecific adsorption, as reported previously. Proteins do adsorb on the PEG surfaces in dynamic equilibrium. The adsorption is more reversible than that on hydrophobic surfaces, which makes the desorption easier upon washing. The first stage of protein adsorption depends neither on surface hydrophobicity nor electrical charge but on molecular diffusion from the bulk phase (high protein concentration) to the surface (zero protein concentration). Affinity comes into play only in the second stage. Our studies have demonstrated that PPEGM was more effective for reduction of nonspecific adsorption than polyethylene glycol.[31,41] Although there are many methods that can be used in the physical adsorption of proteins using nitrocellulose, epoxy, or poly-L-lysine, in those cases it is very difficult to reduce this nonspecific adsorption.

Using the microarray method, it is possible to perform multiple assays at the same time, using a small amount of serum. In the field of allergy diagnosis, 300 μL of serum is usually required to analyze five different allergens in conventional one-to-one assays. However, the microarray system required one-tenth of that amount (30 μL) to analyze five allergens. Integrating the microarray density will increase the number of allergens that can be analyzed. Knecht et al.[57] reported rapid, simultaneous, automated analysis of antibiotics in milk within 5 min. Although our automation system required more than 30 min for measurement of each sample, the data were quantitatively and reproducibly obtained at the level required for clinical diagnosis.

Our study demonstrates that this photoimmobilization technique is useful for multiple simultaneous detection of autoantigen-specific IgG to help diagnosis of autoimmune diseases. The microfluid chip used in the automated system supported the use of very small amounts of sample serum.

Acknowledgment

This study was supported by a grant from the Ministry of Health, Labour, and Welfare of Japan.

Literature Cited

1. Badley EM, Tennant A. Impact of disablement due to rheumatic disorders in a British population; estimates of severity and prevalence from the Calderdale Rheumatic Disablement Survey. *Ann Rheum Dis*. 1993;52:6–13.
2. Jacobson DL, Gange SL, Rose NR, Graham NM. Epidemiology and estimated population burden of selected autoimmune diseases in the United States. *Clin Immunol Immunopathol*. 1997; 84:223–243.
3. Von Muhlen CA, Tan EM. Autoantibodies in the diagnosis of systemic rheumatic diseases. *Semin Arthritis Rheum*. 1995;24: 323–358.

4. Miles J, Charles P, Riches P. A review of methods available for the identification of both organ-specific and non-organ-specific autoantibodies. *Ann Clin Biochem*. 1998;35:19–47.
5. Feng Y, Ke X, Ma R, Chen Y, Hu G, Liu F. Parallel detection of autoantibodies with microarrays in rheumatoid diseases. *Clin Chem*. 2004;50:416–422.
6. Kozarova A, Petrinac S, Ali A, Hudson JW. Array of informatics: Applications in modern research. *J Proteome Res*. 2006; 5:1051–1059.
7. Cretich M, Damin F, Pirri G, Chiari M. Protein and peptide arrays: recent trends and new directions. *Biomol Eng*. 2006;23: 77–88.
8. Chen C-S, Zhu H. Protein microarrays. *BioTechniques*. 2006; 40:423–429.
9. Hu Y, Uttamchandani M, Yao SQ. Microarray: a versatile platform for high-throughput functional proteomics. *Comb Chem High Through Scr*. 2006;9:203–212.
10. Oh SJ, Hong BJ, Choi KY, Park JW. Surface modification for DNA and protein microarrays. *OMICS J Integ Biol*. 2006;10: 327–343.
11. Kingsmore SF. Multiplexed protein measurement: technologies and applications of protein and antibody arrays. *Nat Rev Drug Discov*. 2006;5:310–320.
12. Neuman de Vegvar HE, Amara RR, Steinman L, Utz PJ, Robinson HL, Robinson WH. Microarray profiling of antibody responses against simian-human immunodeficiency virus: post-challenge convergence of reactivities independent of host histocompatibility type and vaccine regimen. *J Virol*. 2003;77: 11125–11138.
13. Mezzasoma L, Bacarese-Hamilton T, Di Cristina M, Rossi R, Bistoni F, Crisanti A. Antigen microarrays for serodiagnosis of infectious diseases. *Clin Chem*. 2002;48:121–130.
14. Kanter JL, Narayana S, Ho PP, Catz I, Warren KG, Sobel RA, Steinman L, Robinson WH. Lipid microarrays identify key mediators of autoimmune brain inflammation. *Nat Med*. 2006; 12:138–143.
15. Bacarese-Hamilton T, Bistoni F, Crisanti A. Protein microarrays: from serodiagnosis to whole proteome scale analysis of the immune response against pathogenic microorganisms. *BioTechniques*. 2002;33:S24–S29.
16. Whiltshire S, O'Malley S, Lambert J, Kukanskis K, Edgar D, Kingsmore SF, Schweitzer B. Detection of multiple allergen-specific IgEs on microarrays by immunoassay with rolling circle amplification. *Clin Chem*. 2000;46:1990–1993.
17. Kim T-E, Park S-K, Cho N-Y, Choi S-Y, Yong T-S, Nahm B-H, Lee S, Noh G. Quantitative measurement of serum allergen-specific IgE on protein chip. *Exp Mol Med*. 2002;34:152–158.
18. Hiller R, Laffer S, Harwanegg C, Huber M, Schmidt WM, Twardosz A, Barletta B, Becker WM, Blaser K, Breiteneder H, Chapman M, Crameri R, Duchene M, Ferreira F, Fiebig H, Hoffmann-Sommergruber K, King TP, Kleber-Janke T, Kurup VP, Lehrer SB, Lidholm J, Muller U, Pini C, Reese G, Scheiner O, Scheynius A, Shen HD, Spitzauer S, Suck R, Swoboda I, Thomas W, Tinghino R, Van Hage-Hamsten M, Virtanen T, Kraft D, Muller MW, Valenta R. Microarrayed allergen molecules: diagnostic gatekeepers for allergy treatment. *FASEB J*. 2002;16:414–416.
19. Fall BI, Eberlein-Koenig B, Behrendt H, Niessner R, Ring J, Weller MG. Microarrays for the screening of allergen-specific IgE in human serum. *Anal Chem*. 2003;75:556–562.
20. Jahn-Schmid B, Harwanegg C, Hiller R, Bohle B, Ebner C, Scheiner O, Mueller MW. Allergen microarray: comparison of microarray using recombinant allergens with conventional diagnostic methods to detect allergen-specific serum immunoglobulin E. *Clin Exp Allergy*. 2003;33:1443–1449.
21. Harwanegg C, Laffer S, Hiller R, Mueller MW, Kraft D, Spitzauer S, Valenta R. Microarrayed recombinant allergens for diagnosis of allergy. *Clin Exp Allergy*. 2003;33:7–13.
22. Harris J, Mason DE, Li J, Burdick KW, Backes BJ, Chen T, Shipway A, Van Heeke G, Gough L, Ghaemmaghami A, Shakib F, Debaene F, Wissinger N. Activity profile of dust mite allergen extract using substrate libraries and functional proteomic microarrays. *Chem Biol*. 2004;11:1361–1372.
23. Deinhofer K, Sevik H, Balic N, Harwanegg C, Hiller R, Rumpold H, Mueller MW, Spitzauer S. Microarrayed allergens for IgE profiling. *Methods*. 2004;32:249–254.
24. Harwanegg C, Hiller R. Protein microarrays in diagnosing IgE-mediated diseases: spotting allergy at the molecular level. *Expert Rev Mol Diagn*. 2004;4:539–548.
25. Benson M, Olsson M, Rudemo M, Wennergren G, Cargelt LO. Pros and cons of microarray technology in allergy research. *Clin Exp Allergy*. 2004;34:1001–1006.
26. Bacarese-Hamilton T, Ardizzoni A, Gray J, Crisanti A. Protein arrays for serodiagnosis of disease. *Methods Mol Biol Protein Arrays*. 2004;264:271–284.
27. Lebrun SJ, Petchpud WN, Hui A, McLaughlin CS. Development of a sensitive, colorometric microarray assay for allergen-responsive human IgE. *J Immunol Methods*. 2005;300:24–31.
28. Woehrl S, Vigl K, Zehetmayer S, Hiller R, Jarisch R, Prinz M, Stingl G, Kopp T. The performance of a component-based allergen-microarray in clinical practice. *Allergy*. 2006;61:633–639.
29. Renault NK, Mirotti L, Alcocer MJC. Biotechnologies in new high-throughput food allergy tests. *Biotechnol Lett*. 2007;29: 333–339.
30. Ott H, Schroeder CM, Stanzel S, Merk H-F, Baron JM. Microarray-based IgE detection in capillary blood samples of patients with atopy. *Allergy*. 2006;61:1146–1152.
31. Ohyama K, Omura K, Ito Y. A Photo-immobilized Allergen microarray for screening of allergen-specific IgE. *Allergol Int*. 2005;54:627–631.
32. Robinson WH, DiGennaro C, Hueber W, Haab BB, Kamachi M, Dean EJ, Fournel S, Fong D, Genovese MC, de Vegvar HE, Skriner K, Hirschberg DL, Morris RI, Muller S, Pruijn GJ, van Venrooij WJ, Smolen JS, Brown PO, Steinman L, Utz PJ. Autoantigen microarrays for multiplex characterization of autoantibody responses. *Nat Med*. 2002;8:295–301.
33. Robinson WH, Fontoura P, Lee BJ, de Vegvar HE, Tom J, Pedotti R, DiGennaro CD, Mitchell DJ, Fong D, Ho PP, Ruiz PJ, Maverakis E, Stevens DB, Bernard CC, Martin R, Kuchroo VK, van Noort JM, Genain CP, Amor S, Olsson T, Utz PJ, Garren H, Steinman LW. Protein microarrays guide tolerizing DNA vaccine treatment of autoimmune encephalomyelitis. *Nat Biotechnol*. 2003;21:1033–1039.
34. Fathman CG, Soares L, Chan SM, Utz PJ. An array possibilities for the study of autoimmunity. *Nature*. 2005;345:605–611.
35. Utz PJ. Protein arrays for studying blood cells and their secreted products. *Immunol Rev*. 2005;204:264–282.
36. Graham KL, Vaysberg M, Kuo A, Utz PJ. Autoantigen arrays for multiplex analysis of antibody isotypes. *Proteomics*. 2006;6: 5720–5724.
37. Kattah MG, Alemi GR, Thibault DL, Balboni I, Utz PJ. A new two-color Fab labeling method for autoantigen protein microarrays. *Nat Methods*. 2006;3:745–751.
38. Lueking A, Possling A, Huber O, Beveridge A, Horn M, Eickhoff H, Schuchardt J, Lehrach H, Cahill DJ. A nonredundant human protein chip for antibody screening and serum profiling. *Mol Cell Proteomics*. 2003;2:1342–1349.
39. Leuking A, Huber O, Wirths C, Schulte K, Stieler KM, Blume-Peytavi U, Kowald A, Hensel-Wiegel K, Tauber R, Lehrach H, Mayer HE, Cahill DJ. Profiling of alopecia areata autoantigens based on protein microarray technology. *Mol Cell Proteomics*. 2005;4:1382–1390.
40. Robinson WH. Antigen arrays for antibody profiling. *Curr Opin Chem Biol*. 2006;10:67–72.
41. Ito Y. Photoimmobilization for microarrays. *Biotechnol Prog*. 2006;22:924–932.
42. Ito Y, Nogawa M. Preparation of a protein micro-array using a photo-reactive polymer for a cell-adhesion assay. *Biomaterials*. 2003;24:3021–3026.
43. Ito Y, Yamauchi T, Omura K. Development of micro-array biochip using photo-immobilization method. *Kobunshi Ronbunshu*. 2004;61:501–510.
44. Ito Y, Nogawa M, Takeda M, Shibuya T. Photo-reactive polyvinylalcohol for photo-immobilized microarray. *Biomaterials*. 2005;26:211–216.
45. Chevolot Y, Martins J, Milosevic N, Leonard D, Zeng S, Malissard M, Berger EG, Maier P, Mathieu HJ, Grout DHG, Sigrist

H. Immobilisation on polystyrene of diazirine derivatives of mono- and disaccharides: biological activities of modified surfaces. *Bioorg Med Chem.* 2001;9:2943–2953.
46. Kanoh N, Kumashiro S, Simizu S, Kondoh Y, Hatakeyama S, Tashiro H, Osada H. Immobilization of natural products on glass slides by using a photoaffinity reaction and the detection of protein-small-molecule interactions. *Angew Chem Int Ed Engl.* 2003;42:5584–5587.
47. Kanoh N, Kyo M, Inamori K, Ando A, Asami A, Nakao A, Osada H. SPR imaging of photo-cross-linked small-molecule arrays on gold. *Anal Chem.* 2006;78:2226–223.
48. Kanoh N, Asami A, Kawatani M, Honda K, Kumashiro S, Takayama H, Simizu S, Amemiya T, Kondoh Y, Hatakeyama S, Tsuganezawa K, Utata R, Tanaka A, Yokoyama S, Tashiro H, Osada H. Photo-cross-linked small-molecule microarrays as chemical genomic tools for dissecting protein-ligand interactions. *Chem Asian J.* 2006;1:789–797.
49. Rusmini F, Zhong Z, Feijen J. Protein immobilization strategies for protein biochips. *Biomacromolecules.* 2007;8:1775–1789.
50. Pei Z, Yu H, Theurer M, Walden A, Nilsson P, Yan M, Randstroem O. Photogenerated carbohydrate microarrays. *Chem Biol Chem.* 2007;8:166–168.
51. Hermanson GH. *Bioconjugate Techniques.* San Diego: Academic Press; 1996:255–256.
52. Collioud A, Clemence J, Sanger M, Sigrist H. Oriented and covalent immobilization of target molecules to solid supports: synthesis and application of a light-activatable and thiol-reactive cross-linking reagent. *Bioconj Chem.* 1993;4:528–536.
53. Yan M, Cai SX, Wybourne JM, Keana JFW. N-hydroxysuccinimide ester functionalized perfluorophenyl azides as novel photoactive heterobifunctional cross-linking reagents. The covalent immobilization of biomolecules to polymer surfaces. *Bioconj Chem.* 1994;5:151–157.
54. Nahar P, Wali NM, Gandhi RP. Light-induced activation of an inert surface for covalent immobilization of a protein ligand. *Anal Biochem.* 2001;294:148–153.
55. Nivens DA, Conrad DW. Photoactive poly(ethylene glycol) organosilane films for site-specific protein immobilization. *Langmuir.* 2002;18:499–504.
56. Mizutani M, Arnold SC, Matsuda T. Liquid, phenylazide-end-capped copolymers of epsilon-caprolactone and trimethylene carbonate: preparation, photocuring characteristics, and surface layering. *Biomacromolecules.* 2002;3:668–675.
57. Knecht BG, Strasser A, Dietrich R, Maertlbauer E, Niessner R, Weller MG. Automated microarray system For the simultaneous detection of antibiotics in milk. *Anal Chem.* 2004;76:646–654.

Manuscript received Jan. 30, 2008, and revision received July 7, 2008.

BTPR0800374